AEDC-TR-68-57

HIGHER ORDER BOUNDARY-LAYER EFFECTS ON ANALYTIC BODIES OF REVOLUTION

John C. Adams, Jr.
ARO, Inc.

April 1968

VON KÁRMÁN GAS DYNAMICS FACILITY
ARNOLD ENGINEERING DEVELOPMENT CENTER
AIR FORCE SYSTEMS COMMAND
ARNOLD AIR FORCE STATION, TENNESSEE

NOTICES

When U. S. Government drawings specifications, or other data are used for any purpose other than a definitely related Government procurement operation, the Government thereby incurs no responsibility nor any obligation whatsoever, and the fact that the Government may have formulated, furnished, or in any way supplied the said drawings, specifications, or other data, is not to be regarded by implication or otherwise, or in any manner licensing the holder or any other person or corporation, or conveying any rights or permission to manufacture, use, or sell any patented invention that may in any way be related thereto.

Qualified users may obtain copies of this report from the Defense Documentation Center.

References to named commercial products in this report are not to be considered in any sense as an endorsement of the product by the United States Air Force or the Government.

HIGHER ORDER BOUNDARY-LAYER EFFECTS ON ANALYTIC BODIES OF REVOLUTION

John C. Adams, Jr.
ARO, Inc.

AF – AEDC
Arnold AFB Tenn

FOREWORD

The research reported herein was supported by the Arnold Engineering Development Center (AEDC), Air Force Systems Command (AFSC), U. S. Air Force, under Contract No. AF40(600)-1200 with ARO, Inc. (a subsidiary of Sverdrup & Parcel and Associates, Inc.). The work was conducted from September 1966 to September 1967, and the manuscript was submitted for publication on February 14, 1968. The ARO Project No. was VW5819. The work is related to Program Element 6240533F, Project 8953, Task 895303.

This report contains material presented as a paper of the same title at the AGARD Seminar on "Numerical Methods for Viscous Flows" held at the National Physical Laboratory, Teddington, England, September 18-21, 1967.

This technical report has been reviewed and is approved.

Carl E. Simmons
Captain, USAF
Research Division
Directorate of Plans & Technology

Edward R. Feicht
Colonel, USAF
Director of Plans & Technology

ABSTRACT

Results are presented from an investigation into second-order compressible boundary-layer theory applicable to blunt bodies formulated for numerical solution in the transformed plane using an implicit finite difference scheme. Various combinations of second-order effects (external vorticity, displacement, transverse curvature, longitudinal curvature, slip, and temperature jump) are considered for two different bodies: a paraboloid and a hyperboloid of 22.5-deg asymptotic half-angle, in a Mach 10 perfect gas flow under low Reynolds number conditions. It is shown that one should properly interpret second-order vorticity and displacement in a combined sense as a vorticity-displacement interaction; numerical results indicate that such interaction is the dominate second-order effect on the bodies under consideration, especially for the hyperboloid where it becomes a first-order effect. Caution is advised in the application of second-order theory to such bodies since the asymptotic matching conditions between inner and outer flow fields may not remain valid as the boundary-layer grows while the external vortical (entropy) layer decreases in thickness.

CONTENTS

APPENDIXES

I. ILLUSTRATIONS

Figure

NOMENCLATURE

Unless otherwise noted, all nondimensional quantities are denoted by a bar over the symbol.

C_f	skin-friction coefficient $[2\tau_w/\rho_\infty U_\infty^2]$
C_{D_f}	skin-friction drag coefficient referenced to base area
C_{D_p}	pressure drag coefficient referenced to base area
c_p	specific heat at constant pressure
M_∞	free-stream Mach number
N	inner expansion coordinate normal to surface $(\bar{N} = n/\epsilon r_N)$
n	outer expansion coordinate normal to surface $(\bar{n} = n/r_N)$
P	inviscid outer flow pressure $(\bar{P} = P/\rho_\infty U_\infty^2)$
P_o'	free-stream normal shock pitot pressure $(\bar{P}_o' = P_o'/\rho_\infty U_\infty^2)$
Pr	Prandtl number
p	inner flow pressure $(\bar{p} = p/p_\infty U_\infty^2)$
q_w	wall heat flux $(\bar{q}_w = q/\rho_\infty U_\infty^3)$
R	inviscid outer flow density $(\bar{R} = R/\rho_\infty)$
R_e	inviscid outer flow density at edge of boundary layer $(\bar{R}_e = R_e/\rho_\infty)$
Re_∞	Reynolds number based on nose radius and free-stream conditions $[\rho_\infty U_\infty r_N/\mu_\infty]$
r	radius $(\bar{r} = r/r_N)$
r_{eff}	effective body radius $(r_{eff} = r_{eff}/r_N)$
r_N	nose radius
r_s	shock radius $(\bar{r}_s = r_s/r_N)$
r_w	wall radius $(\bar{r}_w = r_w/r_N)$
S'	entropy derivative in the basic inviscid flow $(\bar{S}' = S'/c_p)$
St_∞	Stanton number based on free-stream conditions $[-q_w/\rho_\infty U_\infty c_p(T_o - t_w)]$

s	surface distance measured from stagnation point ($\bar{s} = s/r_N$)
T	inviscid outer flow temperature ($\bar{T} = T/U_\infty{}^2/c_p$)
T_e	inviscid outer flow temperature at edge of boundary layer ($\bar{T}_e = T_e/U_\infty{}^2/c_p$)
T_o	free-stream stagnation temperature ($\bar{T}_o = T_o/U_\infty{}^2/c_p$)
T_{ref}	reference temperature $[(\gamma-1)M_\infty{}^2T_\infty]$
T_∞	free-stream temperature
t	inner flow temperature ($\bar{t} = t/U_\infty{}^2/c_p$)
t_w	wall temperature
U	inviscid outer flow tangential velocity ($\bar{U} = U/U_\infty$)
U_e	inviscid outer flow tangential velocity at edge of boundary layer ($\bar{U}_e = U_e/U_\infty$)
U_∞	free-stream velocity
u	inner flow tangential velocity ($\bar{u} = u/U_\infty$)
V	inviscid outer flow velocity component normal to body surface ($\bar{V} = V/U_\infty$)
v	inner flow velocity component normal to body surface ($\bar{v} = v/U_\infty$)
Z	distance along physical body axis ($\bar{Z} = Z/r_N$)
Z_{eff}	distance along effective body axis ($\bar{Z}_{eff} = Z_{eff}/r_N$)
γ	ratio of specific heats
δ	boundary-layer thickness (at $u_1/U_e = 0.995$) ($\bar{\delta} = \delta/r_N$)
δ^*	boundary-layer displacement thickness ($\bar{\delta}^* = \delta^*/\epsilon r_N$)
δ^*_o	boundary-layer displacement thickness at stagnation point ($\bar{\delta}^*_o = \delta^*_o/\epsilon r_N$)
ϵ	Van Dyke's expansion parameter $[(\mu_{ref}/\rho_\infty U_\infty r_N)^{1/2}]$
θ	physical body angle
θ_{eff}	effective body angle
κ	longitudinal surface curvature ($\bar{\kappa} = \kappa/r_N$)

μ	dynamic viscosity ($\bar{\mu} = \mu/\mu_{ref}$)
μ_{ref}	dynamic viscosity evaluated at reference temperature, T_{ref}
ξ, η	transformed Levy-Lees coordinates
ρ	inner flow density ($\bar{\rho} = \rho/\rho_\infty$)
ρ_∞	free-stream density
τ_w	wall shear stress ($\bar{\tau}_w = \tau_w/\rho_\infty U_\infty^2$)

SUBSCRIPTS

o	stagnation conditions
1	first-order quantity
2	second-order quantity
e	at the edge of the boundary layer
eff	effective body quantity
N	at the nose
ref	reference condition
s	at the shock
w	at the physical wall
∞	at free-stream conditions

SECTION I
INTRODUCTION

For several years viscous effects on sharp and blunt-nosed slender bodies at hypersonic speeds have been investigated, both experimentally and theoretically, by the von Kármán Gas Dynamics Facility of the Arnold Engineering Development Center [1-2]. These studies indicate a large viscous-induced drag increment at zero lift which can not be fully explained using results from "classical" first-order boundary-layer theory; an excellent discussion of this limitation is given by Lewis and Whitfield [3] who conclude that further research is needed toward extending the range of applicability of thin boundary-layer theory and inclusion of second-order effects. In pursuing these recommendations attention has been directed to the second-order compressible boundary-layer theory derived by Van Dyke [4]. Basically, Van Dyke's approach involves solving first- and second-order boundary-layer equations which are found from the complete Navier-Stokes equations by an expansion in inverse powers of the square-root of a Reynolds number. The expansion procedure used is the method of inner and outer expansions and results in replacing the Navier-Stokes equations by two separate sets of equations, one set which is valid in the outer inviscid region and another set which is valid in the inner viscous (boundary-layer) region. By using Van Dyke's perturbation procedure the resulting second-order boundary-layer equations are linear and can be subdivided to exhibit several second-order boundary-layer effects, namely displacement, external vorticity, longitudinal curvature, transverse curvature, slip, and temperature jump. We are interested in applying this theory in flow regimes where the expansion parameter ϵ is small but not so small that second-order terms in the parameter are negligible.

Numerous authors in addition to Van Dyke, e.g., Lenard [5], Maslen [6], and Davis and Flügge-Lotz [7], have obtained second-order boundary-layer solutions which are valid only in the stagnation-point region. The work by Davis and Flügge-Lotz [8] represents the first attempt at solution of the second-order boundary-layer equations in regions removed from the nose. They employ an implicit finite-difference method and consider all second-order effects so that the resultant solutions represent a complete first- and second-order boundary-layer theory. They march the finite-difference solutions along the body surface and terminate them several nose radii downstream of the stagnation point; three different analytic bodies are considered, a paraboloid, a hyperboloid (22.5° asymptotic half-angle), and a sphere. The case of flow over the hyperboloid exhibits strong growth of vorticity interaction as the computation proceeds downstream and indicates that the effect of vorticity interaction will become a first-order effect at distances far downstream from the nose. This result is very interesting in that significant vorticity effects may be expected on certain slender blunt-nosed bodies which in turn can now be analyzed using this method.

*Numbers in brackets refer to references on page 12.

SECTION II
THEORETICAL CONSIDERATIONS AND DESCRIPTION OF COMPUTER PROGRAM

In view of the ability of second-order boundary-layer theory to sort out the various second-order effects and their contribution to such quantities of interest as the viscous-induced drag increment, considerable attention has been devoted to this mathematical model. A computer program has been formulated to solve the governing first- and second-order boundary-layer equations in physical variables using the implicit finite-difference scheme of Davis and Flügge-Lotz discussed previously. Any combination of second-order effects may be considered for a specified body geometry; however, the pressure distribution along the body surface must be input to the program from a separate source, say an inviscid blunt body and method of characteristics solution.

Experience with this program has revealed several undesirable features connected with regions of strong boundary-layer growth (where an excessive number of points are used in the finite-difference scheme to traverse the boundary-layer). It is interesting to note that Fannelop [9] has encountered precisely the same problem in treating the first-order boundary-layer equations with crossflow. With this deficiency in mind, and recalling that it is often advantageous to work with similarity variables when solving the boundary-layer equations by numerical methods, it was decided to transform the governing first- and second-order boundary-layer equations using the well-known Levy-Lees transformation [10] written in terms of first-order quantities. A computer program similar to that for the physical variables was written to solve the resultant set of transformed equations using a modification of the Davis and Flügge-Lotz implicit finite-difference scheme to account for variable step size along the body in the transformed plane. Provisions were made in the program to allow solutions for either a Sutherland or power viscosity law as well as arbitrary (but constant) Prandtl number and specific heat ratio. The first-order stagnation point solution was obtained by use of a Runge-Kutta-Gill numerical integration routine in conjunction with an iterative correction scheme; all second-order quantities were set equal to zero at the stagnation point, and hence a forward marching of approximately twenty stations with a very small step size was required before the second-order solution became valid. Another feature included in the program was the capability of obtaining a first-order locally similar solution by setting the nonsimilar terms in the governing first-order equations equal to zero. The resultant set of coupled ordinary nonlinear differential equations was then solved by a successive approximation technique coupled to the same implicit finite-difference scheme used for the nonsimilar case. By this approach the accuracy and limitations of the oft-used locally similar approximation can properly be assessed using a common method of solution.

The present investigation is concerned chiefly with analyzing the various second-order boundary-layer effects on two different analytic bodies of revolution, a paraboloid and a hyperboloid (22.5° asymptotic half-angle), at zero angle of attack under typical low density ideal gas tunnel conditions as shown in Table 1. It should be noted that these bodies are identical to those treated by Davis and Flügge-Lotz [8], and hence the present work may be considered as an extension of their work to regions far removed from the nose under representative tunnel flow conditions. A schematic of the physical body geometry as well as the effective body (physical body perturbed by the displacement thickness) is shown in Fig. 1 (Appendix I).

As mentioned earlier the surface pressure distribution must be input to the program from an external source. For the present work modified Newtonian theory as deduced by Lees [11] was adopted for pressure prediction. Comparison with more exact inviscid blunt body and method of characteristics solutions indicated that the modified Newtonian theory was in excellent agreement for the free-stream conditions and body shapes under consideration (see Fig. 2). As discussed by Hayes and Probstein [12] such agreement should be regarded as fortuitous since apparently the centrifugal pressure difference across the shock layer is approximately offset by the effect of the difference between shock angle and body angle. In any respect the Newtonian theory is certainly attractive with respect to simplicity which will prove to be an important factor in treating the second-order displacement effect to be discussed next.

Controversy has arisen in the past over the proper method for treating the second-order vorticity-displacement interaction effect; excellent discussions of this point may be found in the reviews by Van Dyke [13] and Cheng [14]. Following Van Dyke [15] one is free to choose either a "displacement speed" or "displacement pressure" treatment for the separate effects of second-order vorticity and displacement. Basically, the classification of displacement speed means that the second-order pressure gradient term due to vorticity interaction is treated as a vorticity effect in the second-order tangential momentum equation while displacement pressure means that this pressure gradient term is considered as a displacement effect. Various authors have said that this term does not exist or that it is negligible, while other authors have said that it exists and then fail to include it. The question has been answered in the affirmative by Van Dyke [13] who shows in a very clear manner that this term does indeed exist and should properly be included in any second-order analysis. However, as speculated by Cheng [14], Van Dyke's classification of displacement speed should result in giving the second-order displacement and vorticity effects an unduly large value which is not representative of the actual magnitude for flows over blunt bodies. That such is indeed true is shown in Appendix II where it is concluded that one should properly interpret second-order vorticity and displacement as a combined effect (vorticity-displacement interaction). Such an approach will be followed in the present

work; however, results showing the separate effects of second-order vorticity and displacement treated in a displacement speed sense will also be presented. As discussed in Appendix II this type of treatment is the only correct procedure for analyzing these separate effects using the second-order boundary-layer theory of Van Dyke [4].

As the method of Davis and Flügge-Lotz [8] used in Appendix II is limited in applicability to the extreme nose region of the body, attention has been directed toward developing a more general treatment for consideration of second-order displacement effects over the entire body. Appendix III presents the details of a new method based upon first-order inviscid theory and valid over the entire body. This approach is fully compatible with the second-order theory of Van Dyke [4] and hence represents a valuable tool for numerical evaluation of second-order displacement effects.

SECTION III
DISCUSSION OF RESULTS

The results presented in this paper were obtained from an investigation into second-order boundary-layer effects on analytic bodies of revolution at zero angle of attack in a typical low density tunnel flow field. Particular emphasis was placed upon studying the results of different viscosity laws, Prandtl numbers, and type of solution upon various quantities of interest such as the local skin-friction coefficient and Stanton number. The author believes that only in this manner can one properly assess the influence of each of these parameters on the resultant solution.

In this examination of the effect of various viscosity laws upon both first- and second-order boundary-layer solutions, three different relations were considered: Sutherland, square-root, and linear. A comparison of these laws is shown in Fig. 3 where it is seen that the Sutherland law is in excellent agreement with the data of Hansen [16] in the temperature range of current interest. It is important to note that the linear law underpredicts the viscosity (as compared to the Sutherland value) by a substantial amount, approximately 60 percent maximum deviation. The square-root law is seen to be a more accurate relation with respect to the Sutherland law; use of this law results in an overprediction of only 20 percent maximum. One must keep these discrepancies in mind when evaluating the numerical results of this investigation since the choice of viscosity law influences the boundary-layer character to a considerable extent as will now be shown.

In the past many boundary-layer investigations have been conducted under various assumptions, e.g., linear viscosity law, $Pr = 1.0$, locally similar solution, etc., without due consideration as to the effect of these assumptions on the resultant solution. An attempt has been made in the present study to define and clarify some of these effects by considering first-order

boundary-layer solutions on a common body and set of flow conditions with a common method of solution. In this manner various assumptions can be isolated and properly assessed with regard to the resultant solution. A paraboloid body was chosen having a cool wall ($t_w/T_o = 0.20$) in conjunction with the flow conditions shown in Table I (Appendix IV). The results of this investigation are shown in Figs. 4, 5, and 6. With reference to Fig. 4, which shows the first-order local skin-friction coefficient as a function of surface distance, it is seen that the resultant solutions follow the same trend as the viscosity laws in Fig. 3, i.e., the linear law results in a rather severe underprediction while the square-root law overpredicts by a moderate amount as compared to the Sutherland law. These trends are also valid with respect to the first-order local Stanton number as reference to Fig. 5 will show. Changing the Prandtl number from 0.70 to 1.0 has a very small influence on the skin-friction coefficient and a slightly larger influence on the local Stanton number; note that this effect increases the local skin-friction coefficient and decreases the local Stanton number. Such is reasonable when one recalls that the Prandtl number partially controls the ratio of viscous shear work to thermal heat conduction. The effect of the locally similar approximation is also very small as compared to the complete nonsimilar solution; Fig. 4 shows that the difference in type of solution has almost the same effect as changing the Prandtl number in the nonsimilar solution. However, reference to Fig. 5 shows that the locally similar approximation results in an overprediction of the local Stanton number which is very comparable with the full nonsimilar solution using a square-root viscosity law. It is interesting to note that one of the most oft-used assumptions in classical boundary-layer treatments, namely linear viscosity law, Pr = 1.0, and locally similar solution, results in excellent agreement with the complete nonsimilar solution for Pr = 0.70 and linear viscosity law. Such explains the success of many previous investigations using this type of treatment.

One of the most sensitive boundary-layer quantities is the displacement thickness. Hence, it is certainly of interest to examine it in some detail for the bodies and flow conditions under present examination. The results for first-order displacement thickness are presented in Fig. 6 where the two-dimensional form of the first-order displacement thickness as defined by Eq. (2.33), Davis and Flügge-Lotz [8], has been used in all calculations. For comparison purposes results are presented for both the paraboloid and hyperboloid bodies under both hot and cold wall conditions. Again, the square-root law results in a moderate overprediction while the linear law underpredicts by a substantial amount. The large influence of Prandtl number in changing from 0.70 to 1.0 is rather surprising; however, one must again remember that the Prandtl number effectively controls the ratio of viscous shear work to thermal heat conduction and hence a change in Prandtl number results in a redistribution of both the velocity and temperature profiles which in turn control the displacement thickness. One also notes a similar trend to that found previously in changing from nonsimilar to locally similar solution,

namely the locally similar solution with Pr = 0.70 agrees very well with the nonsimilar solution having Pr = 1.0. Another interesting point to note is that the locally similar solution with Pr = 1.0 and linear viscosity law agrees very well with the nonsimilar solution having Pr = 0.70 and Sutherland viscosity law. Such agreement must be regarded as fortuitous. In comparing the relative displacement thicknesses between the paraboloid and hyperboloid it is seen that the paraboloid has a much larger value. Furthermore, the displacement thickness growth rate is both larger and of different character on the paraboloid as compared to the hyperboloid. Such is a direct consequence of the different body types with the resultant difference in surface pressure distributions as shown in Fig. 2. These factors have a controlling influence on the first-order boundary-layer development and hence control the displacement thickness distribution as well. Noting from Fig. 2 that the paraboloid possesses an always favorable pressure gradient as well as a lower pressure level as compared to the hyperboloid, the above behavior is reasonable to expect since low pressure regions coupled with favorable pressure gradients result in rapid boundary-layer growth. A rather large wall temperature dependence is seen in Fig. 6, especially for the paraboloid; such is to be expected.

Turning now to consideration of second-order boundary-layer effects, one sees in Figs. 7 and 8 the results in terms of first-order and combined first- and second-order theory. Both bodies under consideration are included as well as both hot and cold wall conditions; all second-order effects are included in the combined first- and second-order results so as to represent the aggregate departure from first-order boundary-layer theory. With reference to Fig. 7 several interesting features must be examined. Note that in the nose region ($s/r_N < 1.5$) the local skin-friction coefficient for the paraboloid is higher than for the hyperboloid at the same wall temperature condition. However, such is not true on the aft portion of the body where the hyperboloid has the larger local skin-friction coefficient. Furthermore, note that the first-order curves for the hyperboloid cross at $s/r_N \approx 5.5$ and thence the cool wall has a higher local skin-friction coefficient than does the hot wall. Such is not the case for the paraboloid where the hot wall always has the higher value. This phenomenon is again due to the difference in surface pressure distribution between the two bodies as has been discussed previously. The surface pressure on the hyperboloid reaches an essentially constant value on the aft portion of the body so that the boundary-layer development in this region should be similar to that on a flat plate. Reference to Fig. 3 of the work by Van Driest [17] for compressible flow over a flat plate shows that indeed the skin-friction coefficient for a cold wall is higher than for a hot wall; thus the above premise is certainly reasonable to accept for explaining the apparent discrepancy in results for the two bodies. Such is an extremely interesting effect which should occur on other types of geometry, especially the sphere-cone, providing that the boundary-layer remains laminar.

The local Stanton number distribution as shown in Fig. 8 reveals the same trend as above, namely the local heat flux on the hyperboloid is higher than on the paraboloid over the aft portion of the body. This is in agreement with the results of Fig. 7 through Reynolds analogy ($C_{f_\infty} \propto St_\infty$) which should be applicable in this region.

One notes in Figs. 7 and 8 the striking influence of second-order effects, especially on the local skin-friction coefficient for the hyperboloid. It is seen that the influence of all second-order effects included concurrently represents a perturbation on the first-order results for the paraboloid; such is obviously not the case for the hyperboloid where the second-order effects dominate by far the first-order results. In order to properly interpret these results one must in turn examine each second-order effect considered separately over the entire body range of interest. Figures 9 through 12 present such information for both bodies under both wall conditions. With respect to the increment in the local skin-friction coefficient as shown in Figs. 9 and 11, vorticity-displacement interaction is by far the dominant second-order effect. Note that the vorticity continues to grow with increasing distance along the hyperboloid; however, as pointed out in Appendix II, one must consider vorticity and displacement in a combined sense (vorticity-displacement interaction) when interpreting results. Hence, the displacement effect will tend to cancel the vorticity effect on the aft portion of the hyperboloid which can be seen in the character of the resultant total curve. Further, note that all other second-order quantities are essentially negligible (transverse curvature has a very small effect) with respect to their influence on the local skin-friction increment. Such is not the case for the paraboloid shown in Fig. 9. Here vorticity-displacement interaction is again the dominant effect; however, the other second-order effects (with the exception of slip and temperature jump) are of importance as can be seen from the resultant total curve. With regard to the local Stanton number increment, one sees in Figs. 10 and 12 that all second-order effects are of the same order of magnitude for both bodies. One notes that here slip and temperature jump effects are of importance in the nose region of both bodies. Furthermore, Fig. 12 shows that vorticity-displacement interaction is rapidly becoming dominant on the aft portion of the hyperboloid.

Based on the above detailed investigation into second-order effects, one can safely say that vorticity-displacement interaction is the dominant factor in second-order boundary-layer theory. However, a word of caution must be injected as to the applicability of second-order theory in general and the present results in particular. It is assumed that the boundary-layer thickness is much smaller than the vortical (entropy layer) thickness so that the boundary conditions at the common boundary obtained by asymptotic matching of the two layers remain valid. Such may not be true on the aft portion of the body, especially for the hyperboloid, since the boundary layer is growing in thickness while the vortical layer is diminishing. What is needed is

a "swallowing-type" boundary-layer analysis or a fully viscous shock-layer treatment of the same problem in order to clearly define where second-order boundary-layer theory becomes inapplicable with respect to position along the body. Such an analysis would permit one to properly assess the present results, especially Fig. 7. In this figure an interesting second-order effect is observed, namely the crossing of the first- and second-order hyperboloid curves at $s/r_N \approx 4.0$. This may be due to the same factors as discussed previously for the crossing of the first-order hyperboloid curves; however, second-order theory may also be inapplicable in this case. This is an excellent example where further research is needed before any definite conclusions can be reached as to the scope and range of applicability of second-order boundary-layer theory.

If one accepts the applicability of the present results over the entire body for purposes of discussion, it is of interest to consider the integrated drag contributions over the bodies in question (20 nose radii in length). Table II shows a comparison of both pressure and skin-friction drag coefficients (referenced to the base area of the body where $s/r_N = 20.0$) for the cool wall paraboloid as influenced by viscosity law, Prandtl number, and type of solution. It is seen from Table II that the pressure and skin-friction drag coefficients are of the same order of magnitude for both first- and second-order results, and hence viscous effects are of equal importance as far as the total body drag is concerned. Note that use of the linear viscosity law leads to a severe underprediction of the skin-friction drag (as compared to the Sutherland law prediction) - 31 percent for the first-order result and 40 percent for the combined first- and second-order result. The square-root viscosity law yields a more accurate representation - overpredicting the skin-friction drag by only 6 percent for the first-order and 9 percent for the combined first- and second-order. Changing the Prandtl number to unity or using a locally similar type solution has an almost negligible influence on the resultant skin-friction drag (less than 2 percent increase in all cases). These differences can be traced back to the local skin-friction coefficient distribution as shown in Fig. 4 and discussed previously. Furthermore, the differences in the first- and second-order drag coefficient due to pressure are directly related to the displacement thickness distributions shown in Fig. 6 since the second-order contribution to the pressure drag is computed from knowing the pressure distribution over the effective body (physical body perturbed by the displacement thickness).

In order to clarify the results of various second-order effects upon the total drag for both the paraboloid and hyperboloid bodies at both wall conditions, one must consult Table III. Considering the paraboloid first, note that both the first-order and combined first- and second-order skin-friction drag increases with increasing wall temperature. With respect to the second-order quantities it is seen that vorticity-displacement interaction and transverse curvature effects are of the same order of magnitude

while longitudinal curvature and slip and temperature jump effects are an order of magnitude smaller. It is apparent that vorticity-displacement interaction is the dominant second-order effect on the skin-friction drag increment; the displacement effect on the second-order pressure drag increment is of equal importance with respect to the magnitude of separate effects. Hence, the second-order results for the paraboloid may indeed be regarded as perturbations on the first-order results with vorticity-displacement interaction as the important second-order effect.

Turning now to the hyperboloid, one observes several interesting differences in Table III. First, it is seen that the first-order and combined first- and second-order skin-friction drag coefficients both decrease with increasing wall temperature; this is due to the curve crossing shown in Fig. 7 and was discussed previously. It is further noted that vorticity-displacement interaction is by far the dominant second-order effect, being two orders of magnitude larger than any of the other second-order effects and of the same order of magnitude as the first-order solutions. In fact, the second-order vorticity-displacement interaction increment on the skin-friction drag coefficient is over twice the value of the first-order skin-friction drag coefficient alone! Hence, the effects of vorticity-displacement interaction are definitely of first-order in numerical magnitude; however, these results must be viewed with caution as to the applicability of second-order theory as discussed previously. Again, the effects of longitudinal curvature and slip and temperature jump are an order of magnitude less than transverse curvature and displacement effects and thus essentially negligible in comparison with the other effects. In summary, one can safely say that the hyperboloid is certainly dominated in the second-order sense by the vorticity-displacement interaction effect.

A few words should be said in conclusion as to the computer time requirements and character of numerical solutions for this investigation. The program itself was written in FORTRAN 63 for solution on a CDC 1604-B computer. Computation time including printout for both first- and second-order equations averaged 8 seconds per station in transformed variables as compared with 10 seconds in physical variables - a 20-percent reduction in time requirements. This time comparison is based upon sphere-cone geometry and not the analytic bodies reported herein; solution time in transformed variables for the analytic bodies also averaged 8 seconds per station with physical variable results not available.

A total of 300 stations was used which resulted in a total time requirement of approximately 45 minutes to complete the calculations for a body of 25 nose radii in length. Using Levy-Lees variables results in the solution being obtained in the transformed (ξ,η) plane; for the present investigation the following step sizes were chosen:

$$\eta_{max} = 6.0$$

$$\Delta\eta = 0.050$$

$$\Delta(s/r_N) = 0.0125,\ 0.0250,\ 0.0500,\ 0.1000$$

where a procedure for doubling the s/r_N step size at any chosen location was built into the program; hence the s/r_N step size was doubled a total of four times over the bodies of interest in this work. Such a step size change procedure is highly advantageous in reducing the total computing time requirements for long bodies. Repetition of the calculations with a halved step size in $\Delta\eta$ as well as an increase in η_{max} to 9.0 showed no change in the numerical results. That the bodies in question are essentially independent of the $\Delta(s/r_N)$ step size is evidenced by the excellent agreement of the locally similar solution (which is independent of this step size). The implicit finite-difference scheme proved to be inherently stable in all cases and any oscillations introduced by the second-order stagnation point treatment were quickly damped out. All in all, the method must be described as highly satisfactory in the numerical sense.

SECTION IV
CONCLUSIONS

The present investigation produced the following results:

1. The first- and second-order compressible boundary-layer theory of Van Dyke [4] coupled with the implicit finite-difference scheme of Davis and Flügge-Lotz [8] written in terms of transformed Levy-Lees variables is an excellent method for treating second-order boundary-layer effects (external vorticity, displacement, transverse curvature, longitudinal curvature, slip, and temperature jump) on blunt-nosed bodies of revolution.

2. Application of this method to two analytic bodies of revolution, a paraboloid and a hyperboloid of 22.5^o asymptotic half-angle, under typical low density tunnel conditions at $M_\infty = 10.0$ in conjunction with perfect gas, constant specific heats, and constant Prandtl number (not necessarily unity) assumptions resulted in a thorough study of first- and second-order boundary-layer effects as influenced by viscosity law, Prandtl number, type of solution, body geometry, and surface pressure distribution.

3. Use of a linear viscosity law results in a rather severe underprediction of the skin friction (and the resultant integrated skin-friction drag) as compared to the Sutherland law; the square-root viscosity law overpredicts the

same quantities by a slight amount, again as compared to the Sutherland law. Effects of changing the Prandtl number from 0.70 to 1.0 are almost negligible with respect to the local skin-friction coefficient and Stanton number distribution on the paraboloid; this change has a surprising influence in increasing the displacement thickness of the boundary-layer over the paraboloid.

4. Comparison of first-order locally similar solutions to the first-order nonsimilar solutions for the paraboloid shows them to be in excellent agreement with regard to prediction of heat-transfer and skin-friction distributions. However, the boundary-layer displacement thickness is overpredicted by the locally similar approximation.

5. Wall temperature has an interesting effect on the hyperboloid in that the cool wall case has a higher skin-friction drag, both first- and second-order, than does the hot wall case. This is explained by "transition" of the boundary-layer to flat plate behavior on the aft portion of the body due to the surface pressure becoming constant.

6. The separate second-order effects of vorticity and displacement must be considered in a displacement speed sense; a displacement pressure treatment is not consistent with the governing second-order equations and matching conditions of Van Dyke [4] in the limiting sense as $\bar{N} \to \infty$. However, a displacement speed treatment is unreasonable with respect to the magnitude of the separate effects and certainly not representative of the actual physical effects. Hence, it is proposed that one should properly interpret second-order vorticity and displacement in a combined sense as a vorticity-displacement interaction. Such is followed in the present investigation.

7. A new and powerful technique for considering the second-order displacement effect using first-order inviscid theory is presented which is in complete accord with the second-order theory of Van Dyke [4]. This approach is not limited to the nose region and and may be applied equally well over the entire body. For the present investigation, modified Newtonian theory is used in conjunction with this new method; however, such may not be strictly valid in that modified Newtonian predictions do not necessarily represent a solution (in a mathematical sense) to the governing first-order outer flow equations of motion. More work is needed in this area to define the limits of error for this type of approach.

8. Vorticity-displacement interaction is by far the dominant second-order boundary-layer effect on both bodies under

consideration. For the paraboloid all second-order effects may be considered as perturbations on the first-order solution. This is not true on the hyperboloid where the second-order vorticity-displacement interaction increment in the skin-friction drag is larger than the first-order contribution. Caution is advisable in the application of second-order perturbation-type theory to such bodies since the asymptotic matching conditions between inner and outer flow fields may not remain valid as the boundary-layer grows while the vortical (entropy) layer decreases in thickness. More work is definitely needed in order to clearly define the range of applicability of second-order boundary-layer theory.

REFERENCES

1. Griffith, B. J. and Lewis, C. H. "Laminar heat transfer to spherically blunted cones at hypersonic conditions," AIAA J. 2, 438-444 (1964).

2. Whitfield, J. D. and Griffith, B. J. "Hypersonic viscous drag effects on blunt slender cones," AIAA J. 2, 1714-1722 (1964).

3. Lewis, C. H. and Whitfield, J. D. "Theoretical and experimental studies of hypersonic viscous effects," AGARDograph 97, Part III, pp. 63-119 (1965).

4. Van Dyke, M. "Second-order compressible boundary-layer theory with application to blunt bodies in hypersonic flow," Hypersonic Flow Research, edited by F. R. Riddell (Academic Press, Inc., New York, 1962), pp. 37-76.

5. Lenard, M. "Stagnation point flow of a variable property fluid at low Reynolds numbers," Thesis, Cornell University, Graduate School of Aeronautical Engineering (1961).

6. Maslen, S. H. "Second-order effects in laminar boundary-layers," AIAA J. 1, 33-40 (1963).

7. Davis, R. T. and Flügge-Lotz, I. "The laminar compressible boundary-layer in the stagnation point region of an axisymmetric blunt body including the second-order effect of vorticity interaction," Int. J. Heat Mass Transfer 7, 341-370 (1964).

8. Davis, R. T. and Flügge-Lotz, I. "Laminar compressible flow past axisymmetric blunt bodies (results of second-order theory)," Stanford University, Division of Engineering Mechanics TR-143 (1963).

9. Fannelop, T. K. "A method of solving the three-dimensional laminar boundary-layer equations with application to a lifting re-entry body," Avco Missile Systems Division BSD-TR-66-209 (1966).

10. Lees, L. "Laminar heat transfer over blunt-nosed bodies at hypersonic flight speeds," Jet Propulsion 26, 259-269, 274 (1956).

11. Lees, L. "Hypersonic flow," Inst. Aero Sci. Preprint No. 554 (1955).

12. Hayes, W. D. and Probstein, R. F. Hypersonic Flow Theory, (Academic Press, Inc., New York, 1959), p. 243.

13. Van Dyke, M. "A review and extension of second-order hypersonic boundary-layer theory," Rarefied Gas Dynamics, Vol. II. Supplement 2, edited by J. A. Lauermann (Academic Press, Inc., New York, 1963), pp. 212-227.

14. Cheng, H. K. "Viscous hypersonic blunt-body problems and the Newtonian theory," Fundamental Phenomena in Hypersonic Flow, edited by J. Gordon Hall (Cornell University Press, Ithaca, New York, 1966), pp. 90-131.

15. Van Dyke, M. "Higher approximations in boundary-layer theory, Part 1," J. Fluid Mechanics 14, 161-177 (1962).

16. Hansen, C. F. "Approximations for the thermodynamic and transport properties of high-temperature air," NASA TR R-50 (1959).

17. Van Driest, E. R. "Investigation of laminar boundary-layer in compressible fluids using the Crocco method," NACA TN 2597 (1952).

18. Lewis, C. H. "First- and second-order boundary-layer effects at hypersonic conditions," Paper presented at AGARD Seminar on "Numerical Methods for Viscous Flows," National Physical Laboratory, Teddington, England, September 18-21, 1967.

APPENDIXES

I. ILLUSTRATIONS

II. VORTICITY-DISPLACEMENT INTERACTION TREATMENT

III. DISPLACEMENT TREATMENT USING EFFECTIVE BODY TECHNIQUE

IV. TABLES

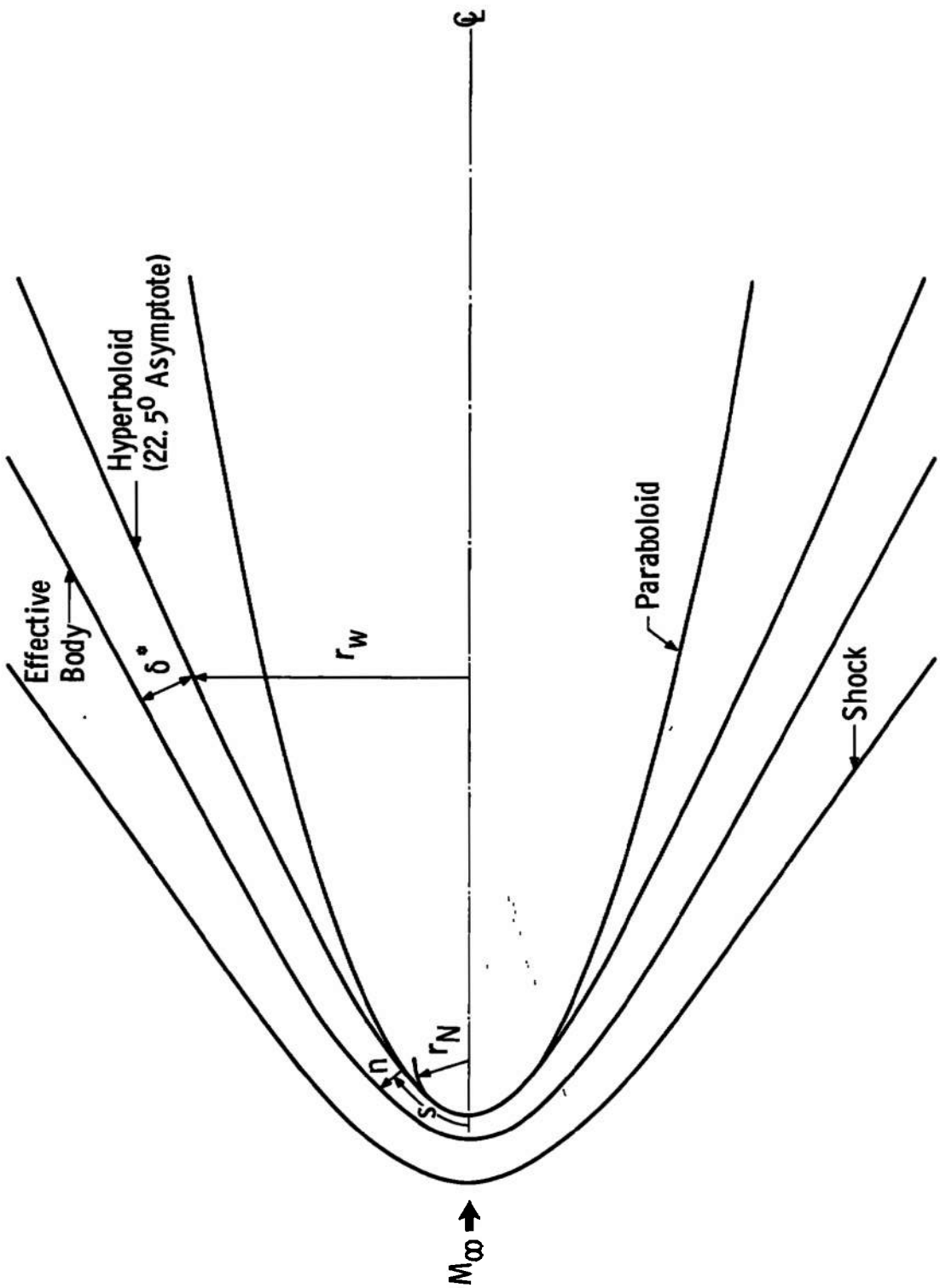

Fig. 1 Schematic of Body Geometry

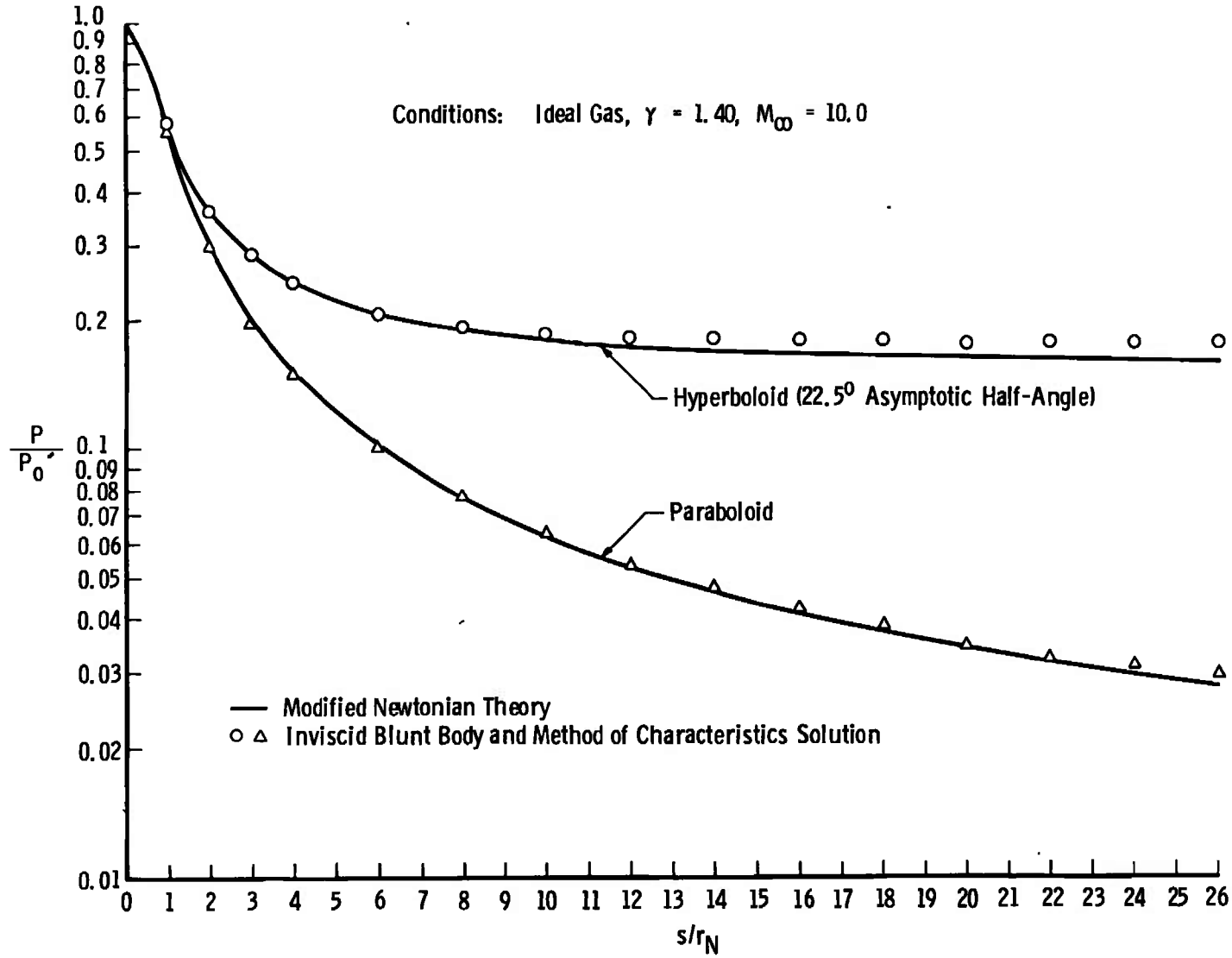

Fig. 2 Surface Pressure Distribution

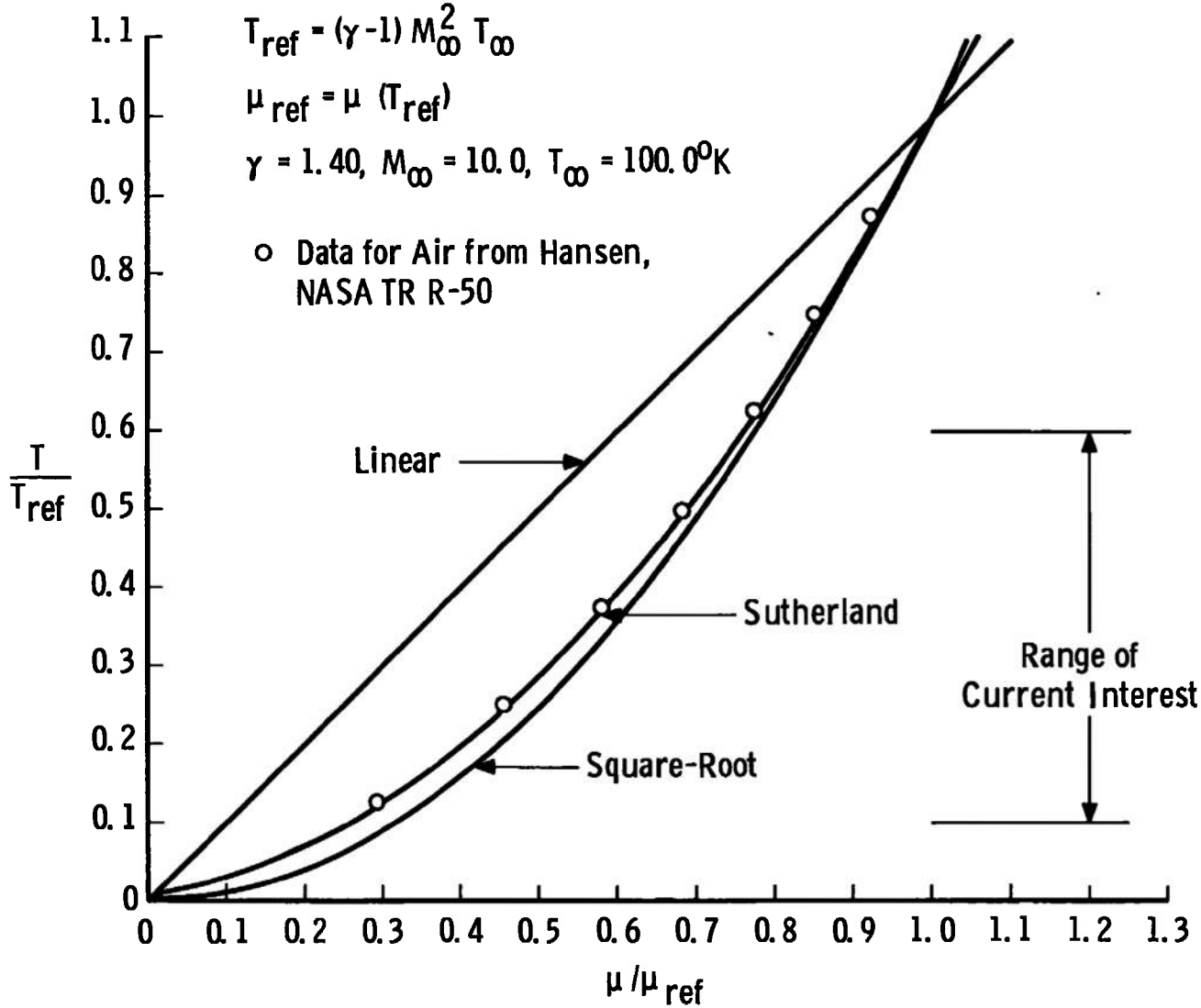

Fig. 3 Comparison of Various Viscosity Laws

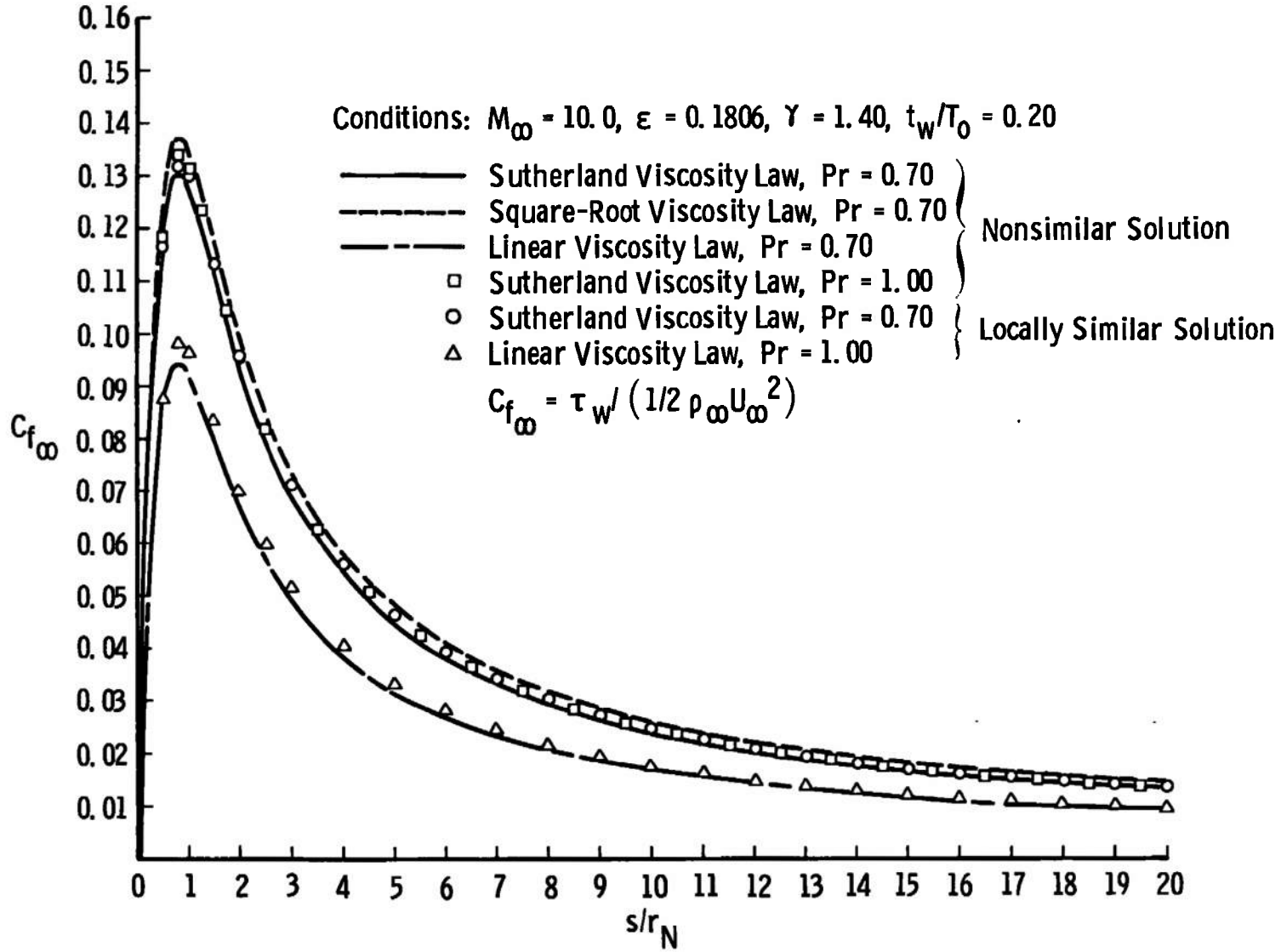

Fig. 4 Comparison of First-Order Local Skin-Friction Coefficients on Paraboloid

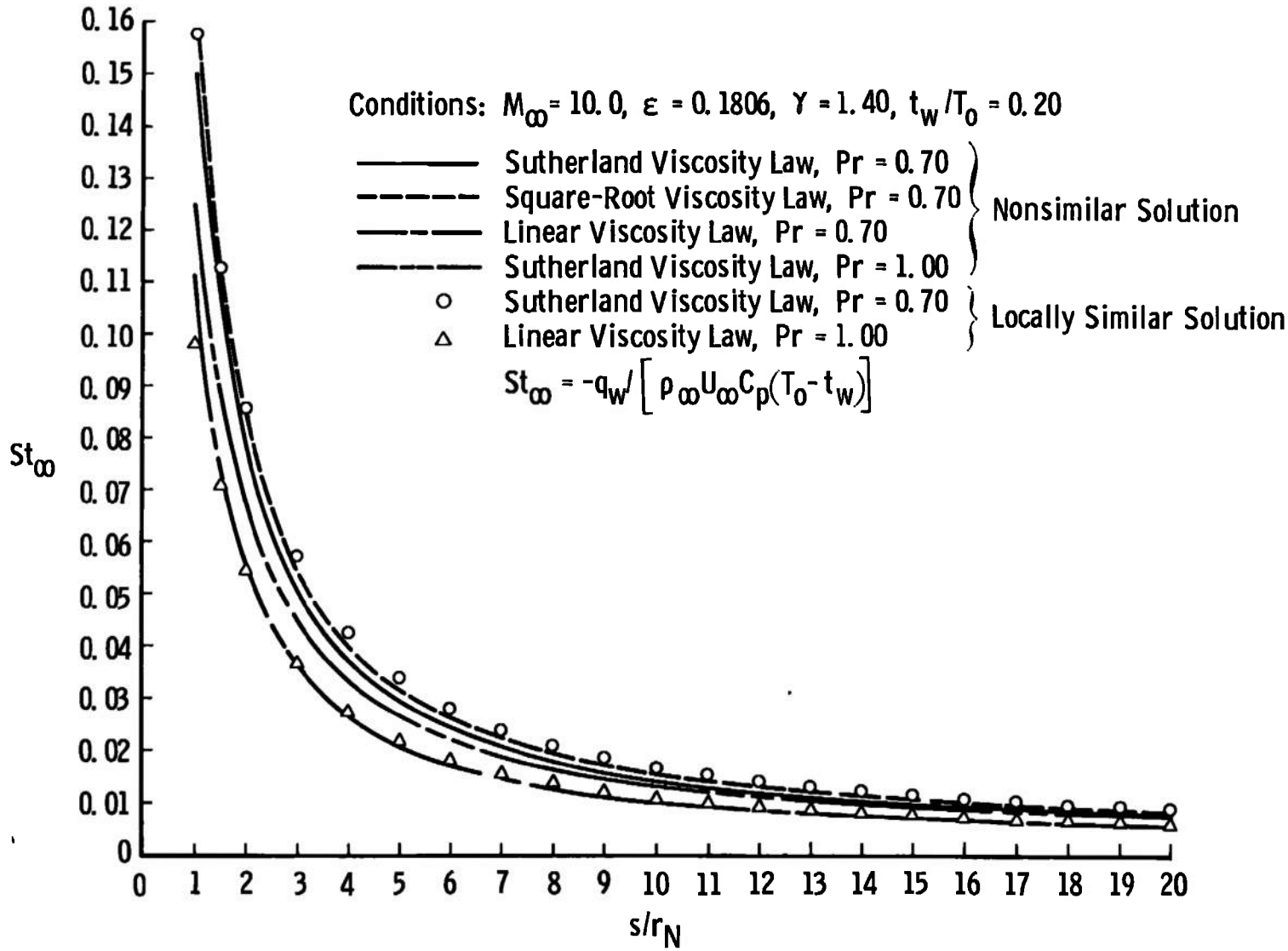

Fig. 5 Comparison of First-Order Local Stanton Numbers on Paraboloid

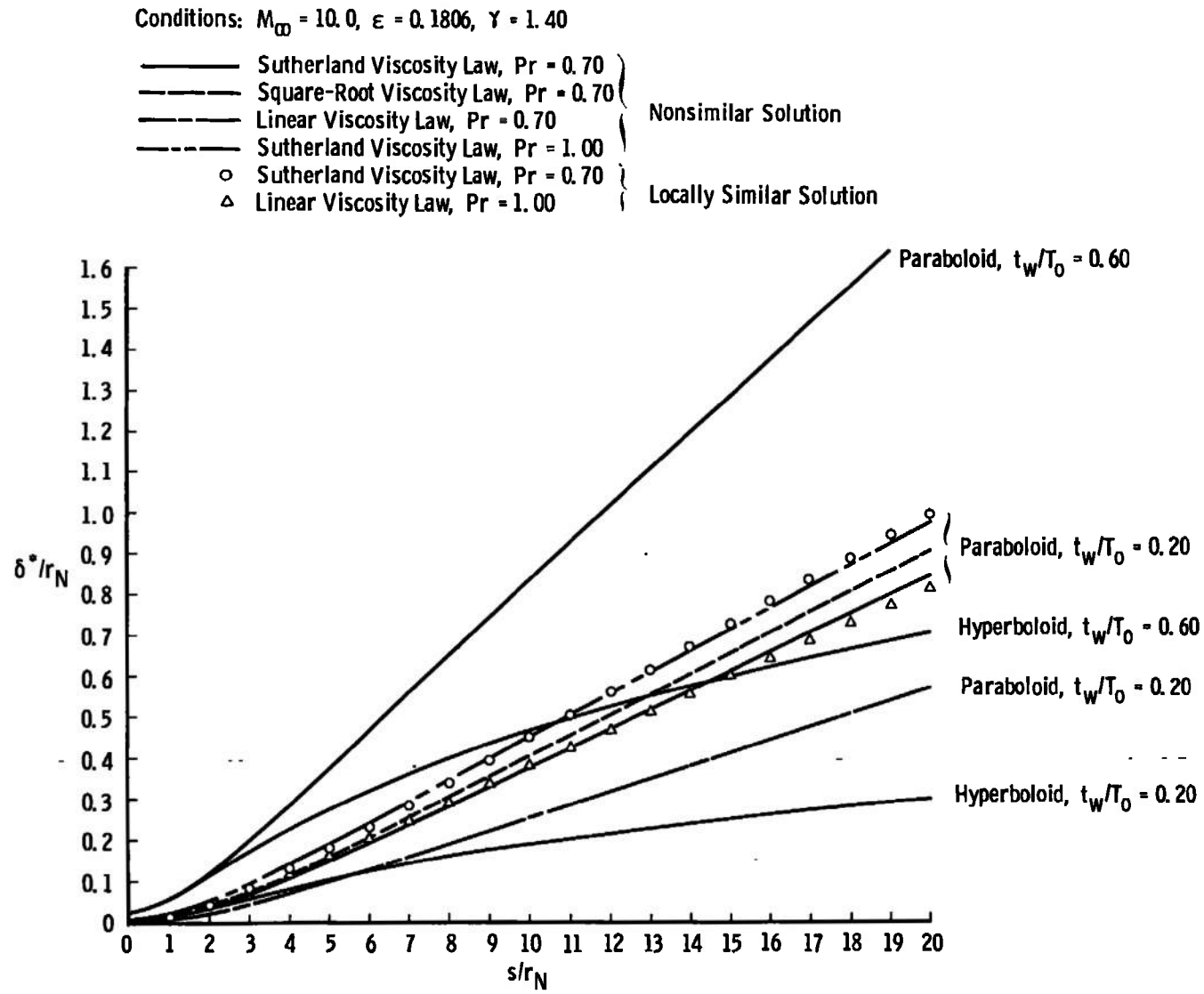

Fig. 6 Comparison of First-Order Displacement Thickness

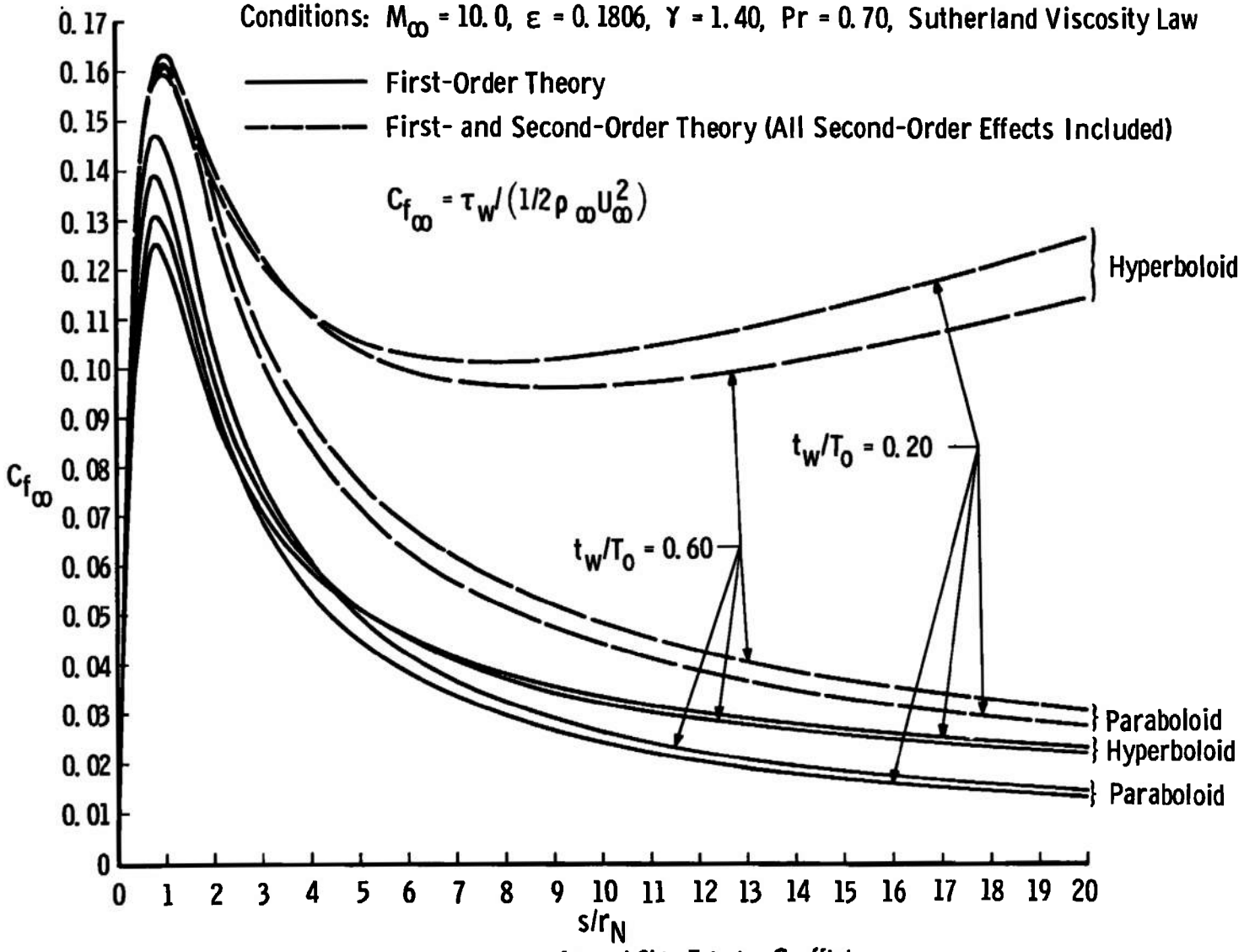

Fig. 7 Comparison of Local Skin-Friction Coefficients

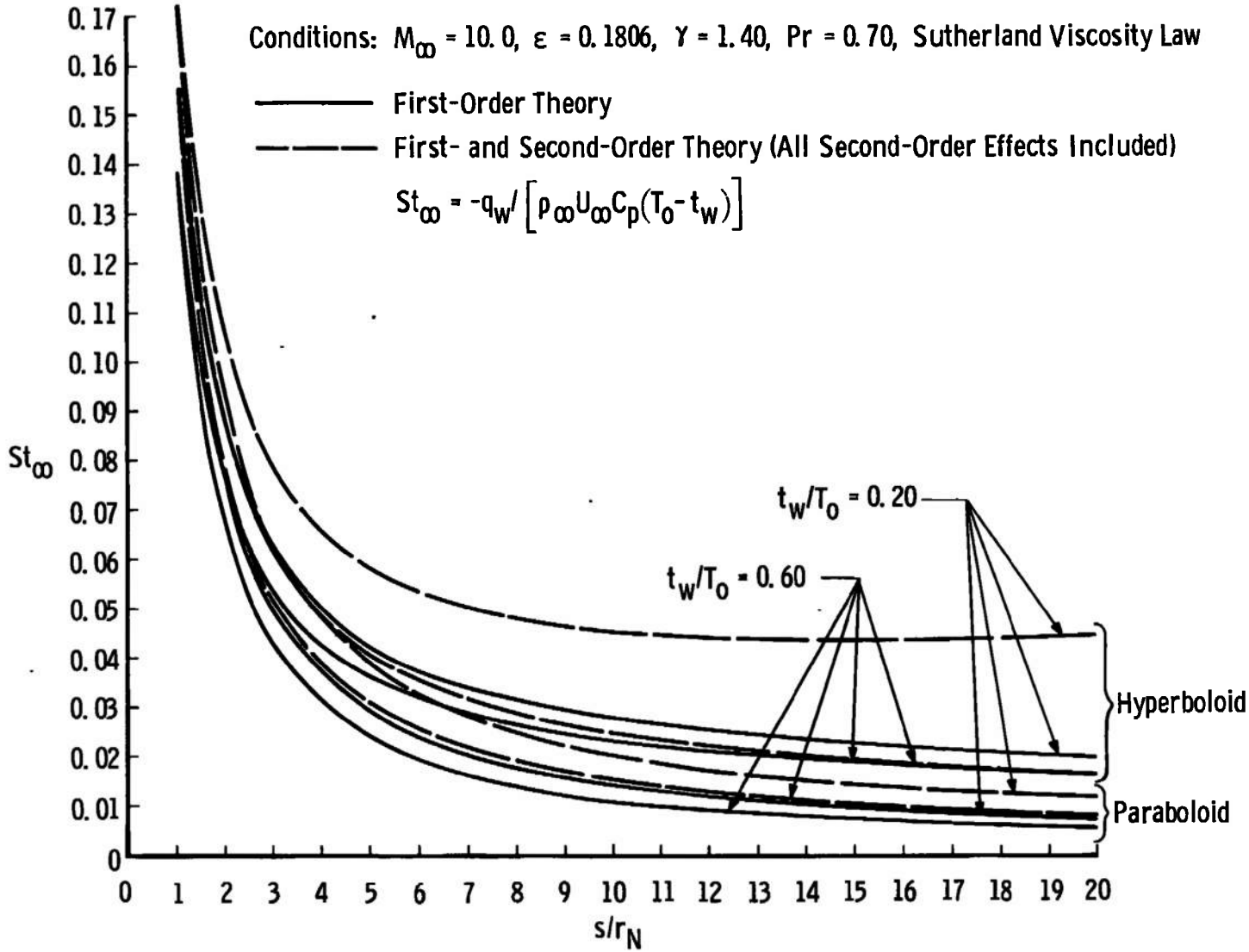

Fig. 8 Comparison of Local Stanton Numbers

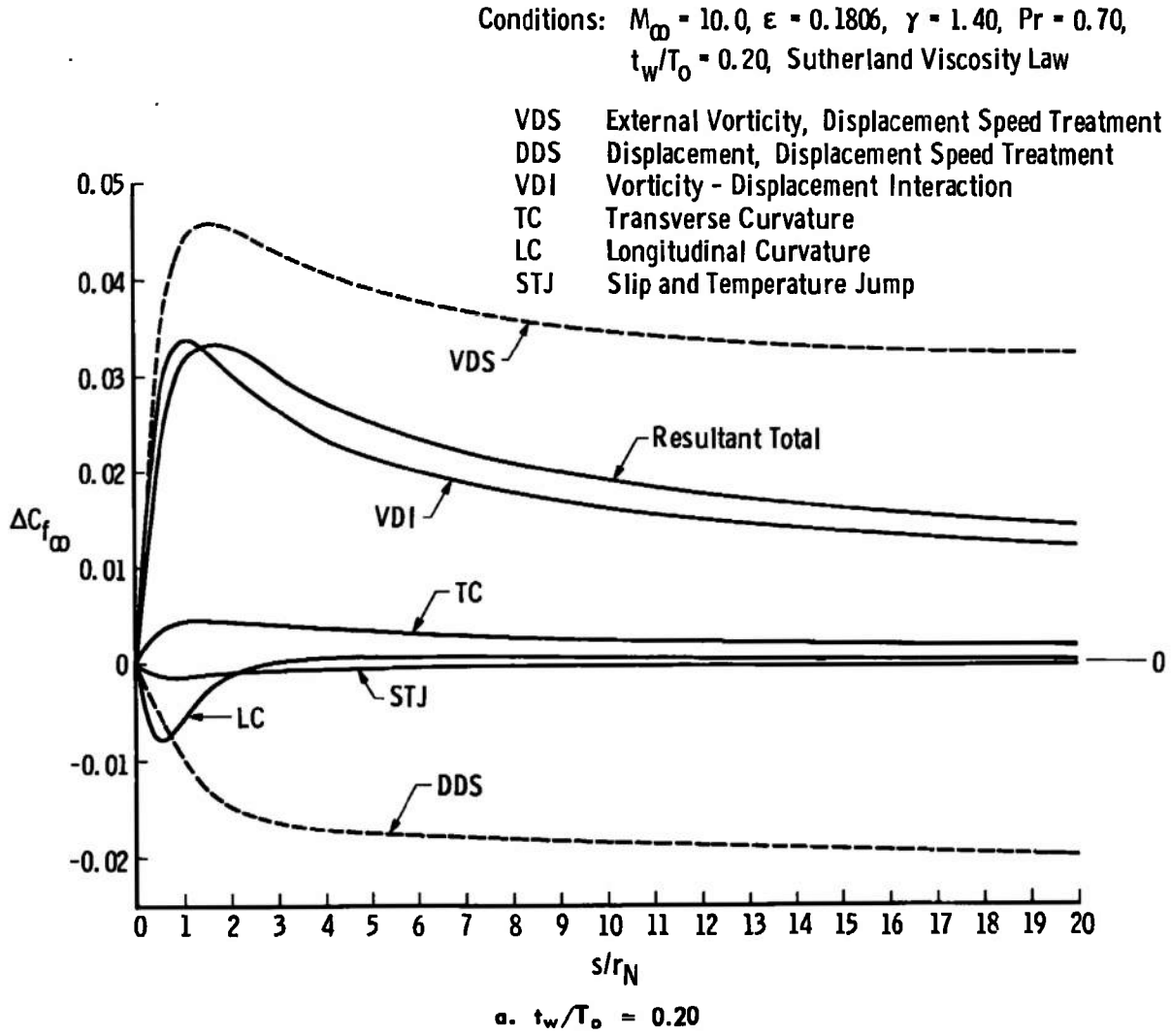

a. t_w/T_o = 0.20

Fig. 9 Increment in Local Skin-Friction Coefficient on Paraboloid due to Second-Order Effects

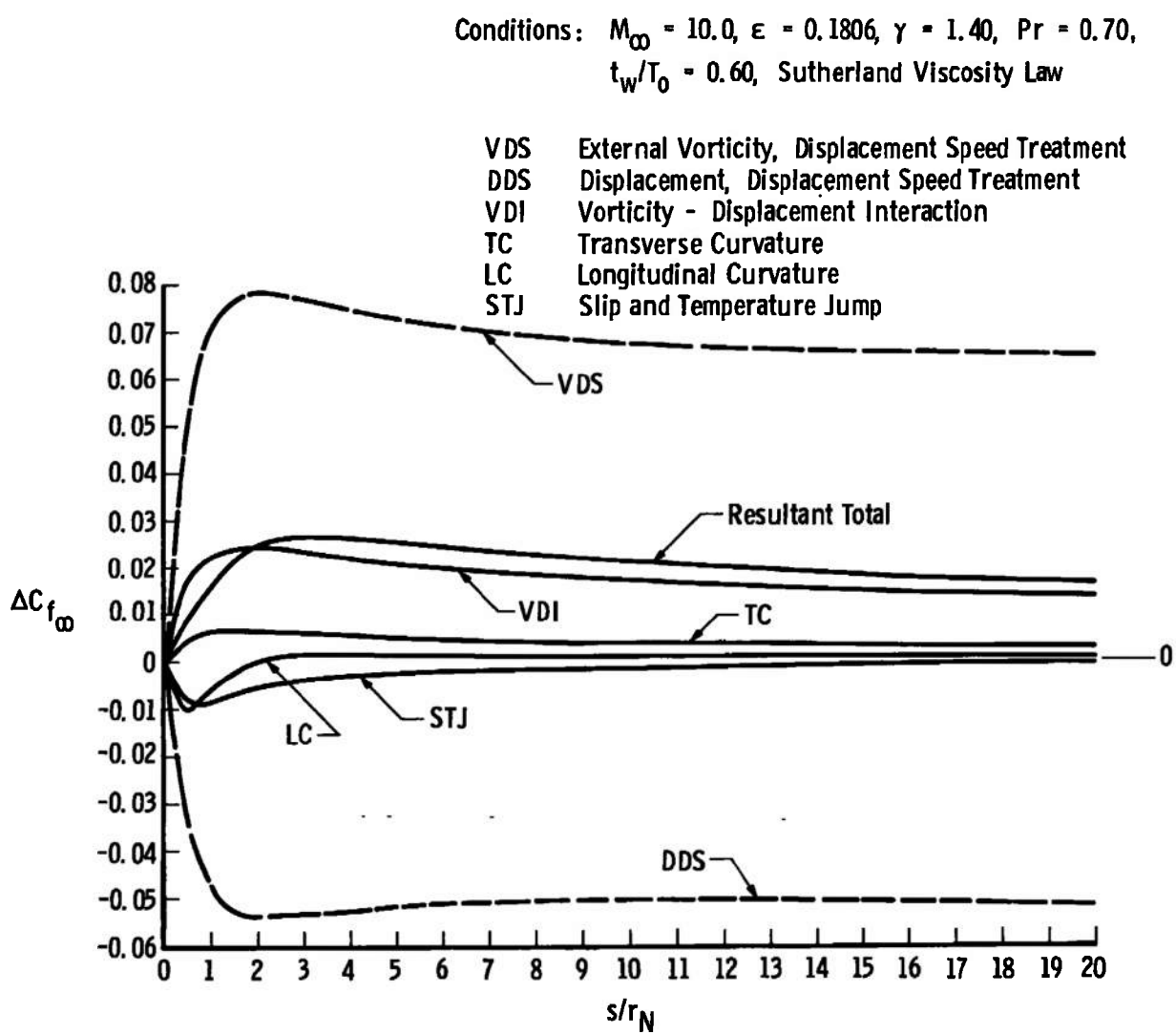

b. t_w/T_o = 0.60

Fig. 9 Concluded

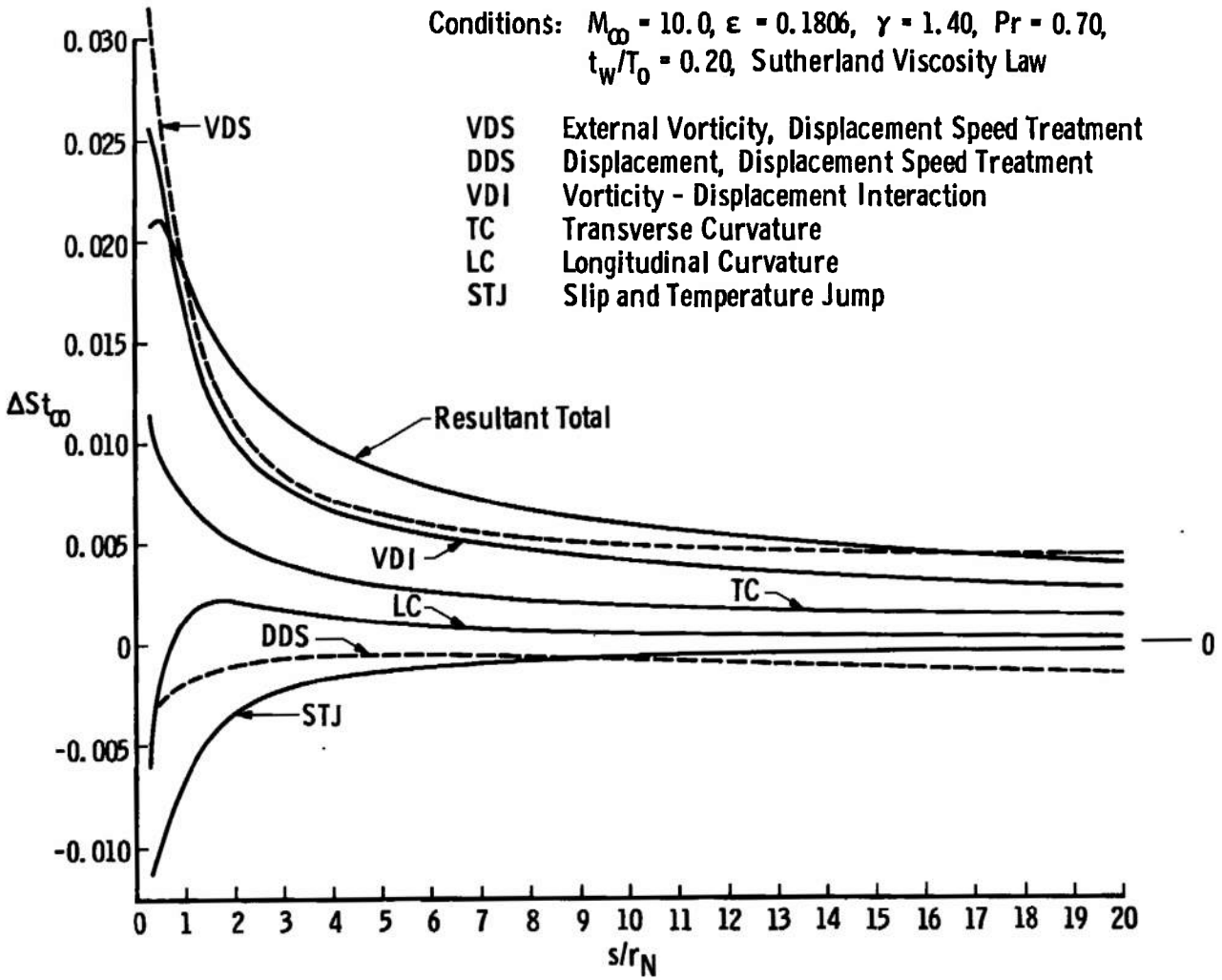

a. t_w/T_o = 0.20

Fig. 10 Increment in Local Stanton Number on Paraboloid due to Second-Order Effects

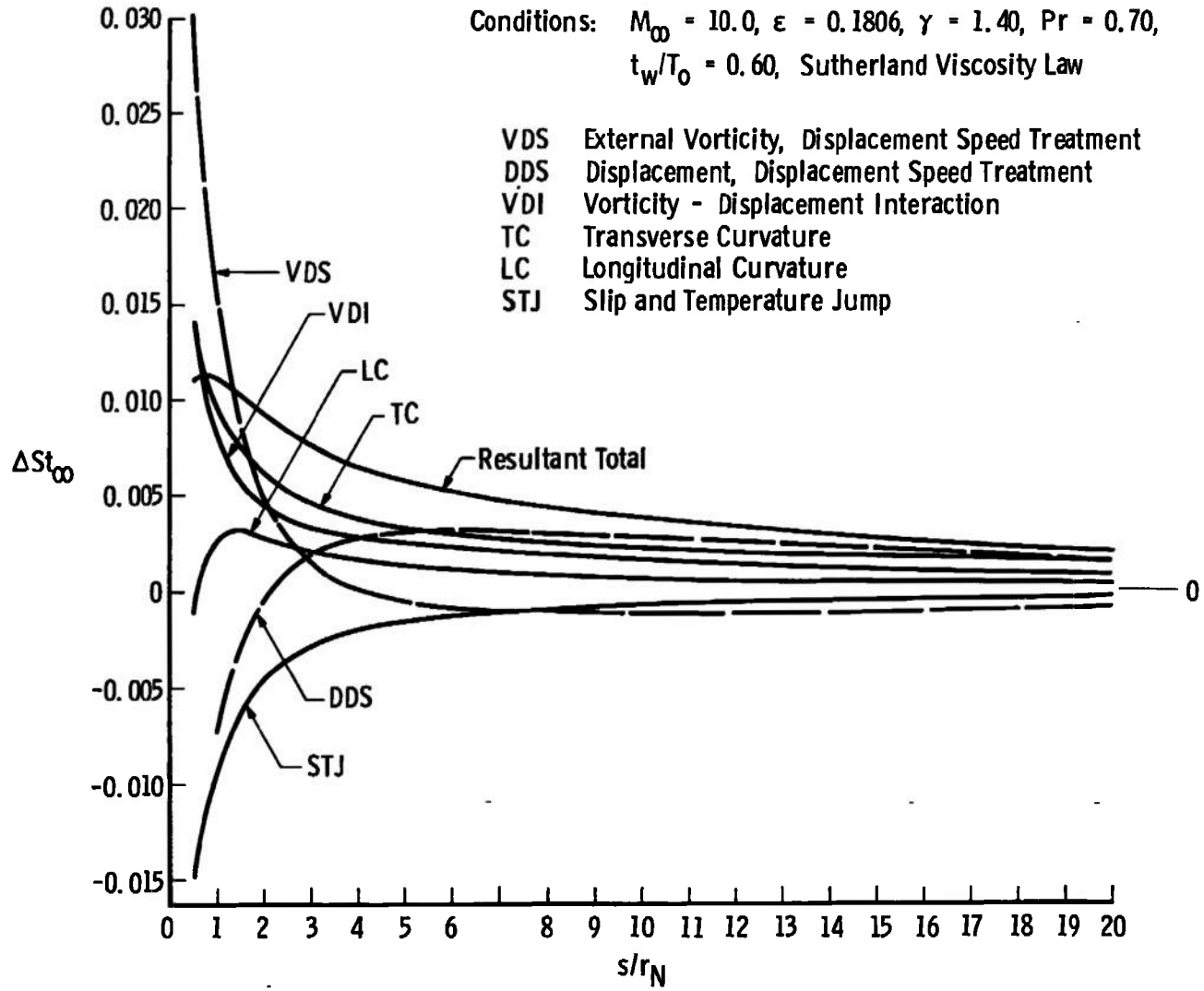

b. t_w/T_o = 0.60

Fig. 10 Concluded

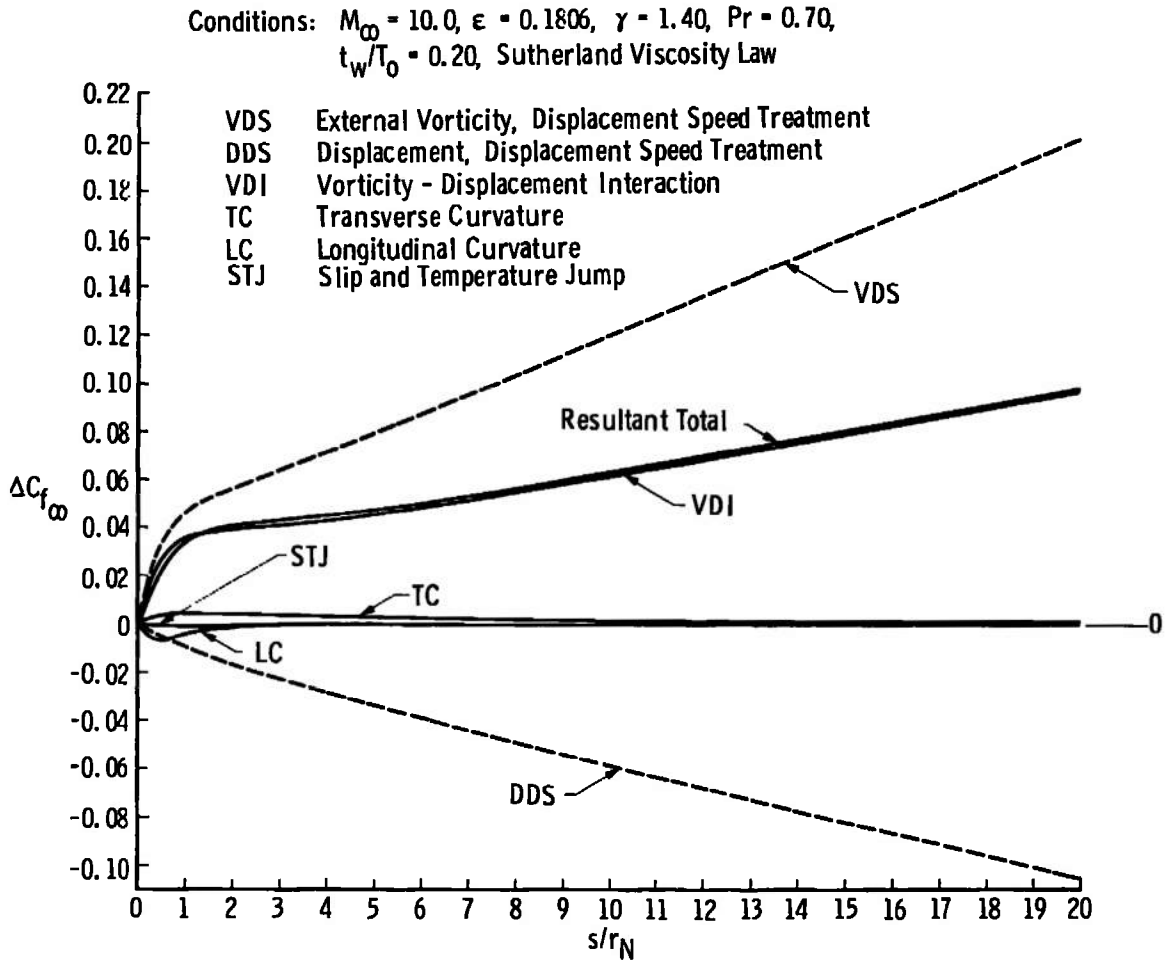

a. t_w/T_o = 0.20

Fig. 11 Increment in Local Skin-Friction Coefficient on Hyperboloid due to Second-Order Effects

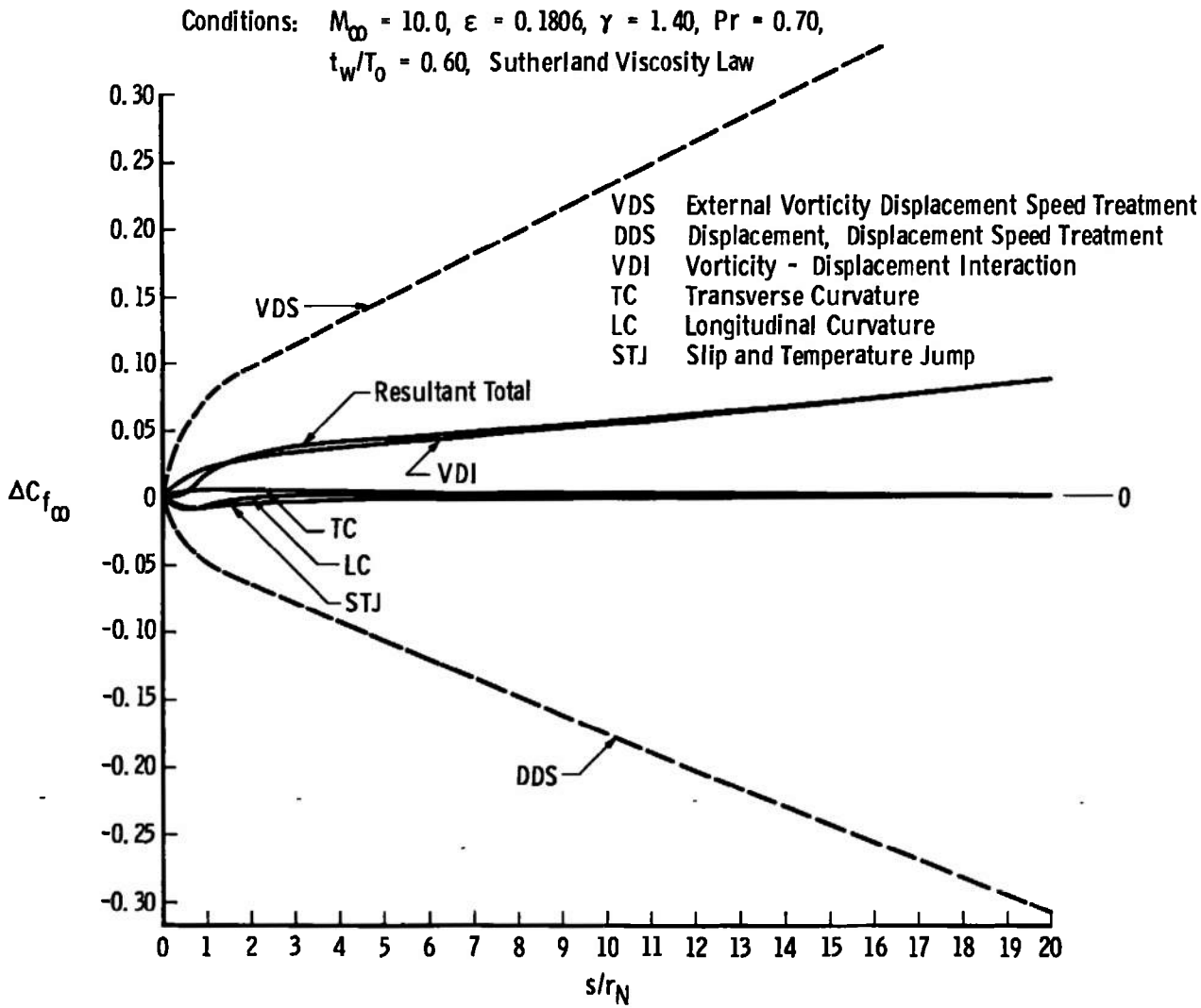

b. t_w/T_o = 0.60

Fig. 11 Concluded

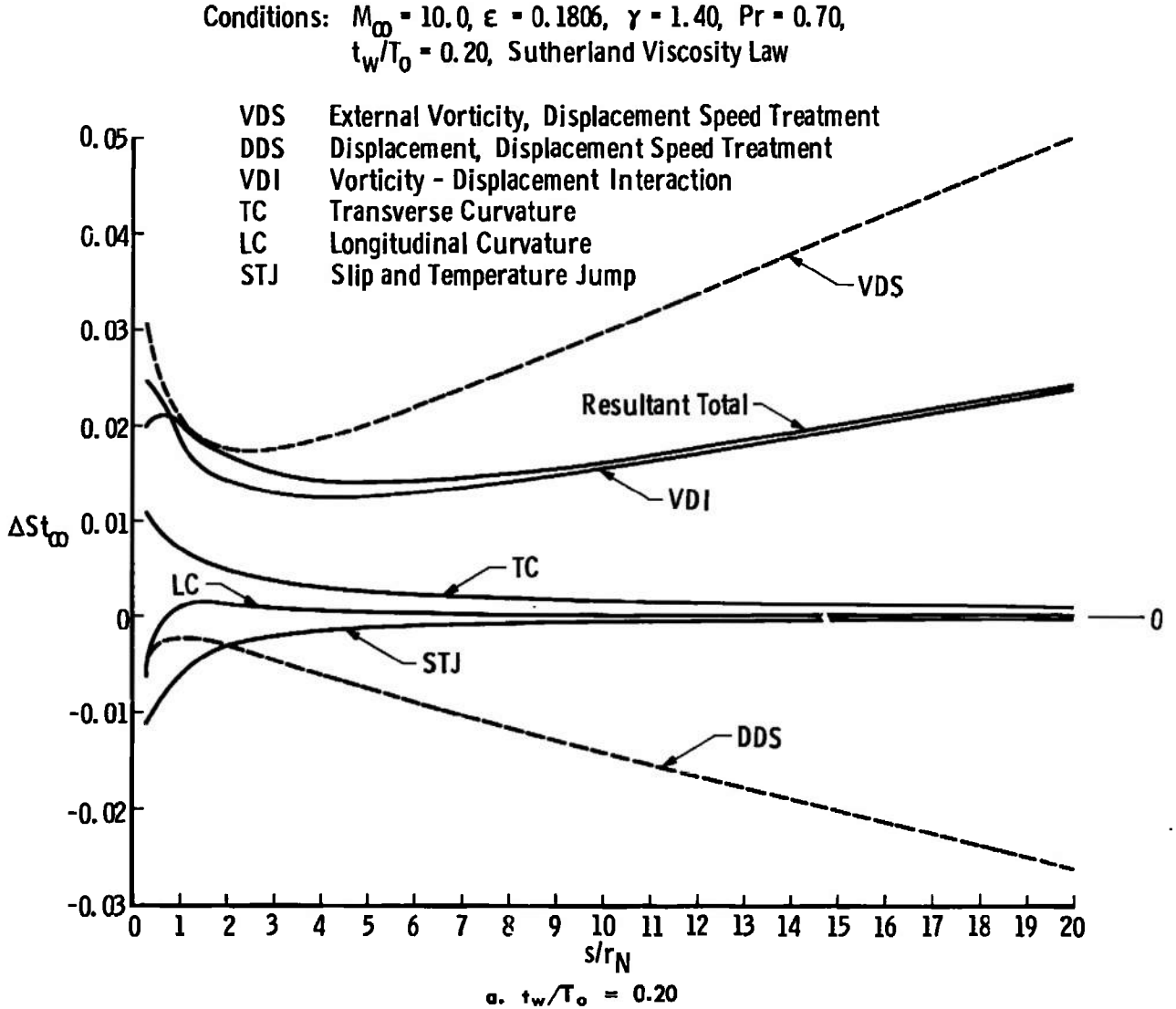

a. t_w/T_o = 0.20

Fig. 12 Increment on Local Stanton Number on Hyperboloid due to Second-Order Effects

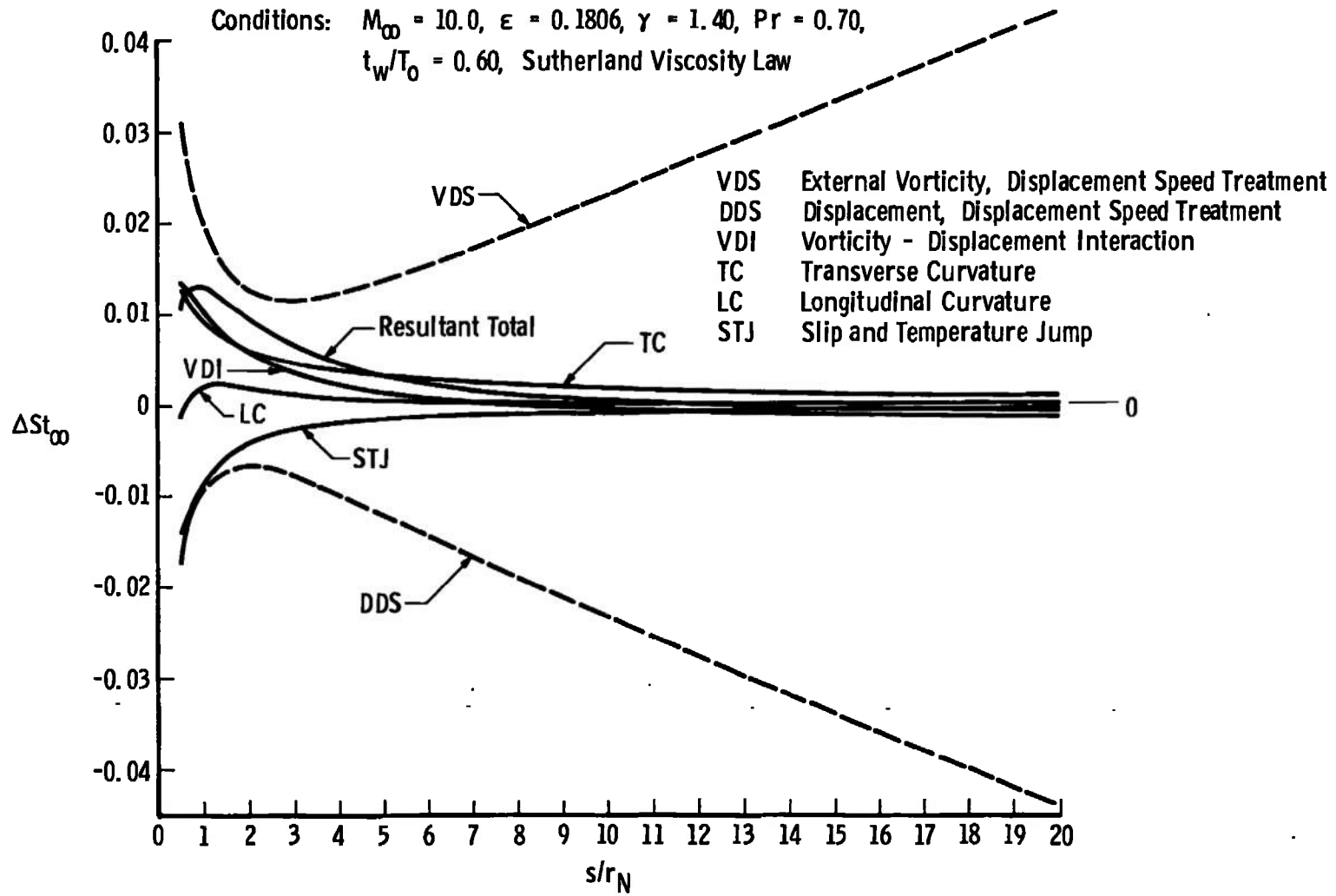

b. t_w/T_o = 0.60

Fig. 12 Concluded

APPENDIX II
VORTICITY-DISPLACEMENT INTERACTION TREATMENT

For checkout purposes using the transformed variables program, solutions were run for a paraboloid and hyperboloid (22.5^{o} asymptotic half-angle) at $\gamma = 1.40$, $Pr = 0.70$, and $M_{\infty} \rightarrow \infty$ for wall-to-stagnation temperature ratios of 0.20 and 0.60 with a square-root viscosity law. These conditions are precisely those used by Davis and Flügge-Lotz [8] and hence enable a direct comparison with their results. Such is extremely valuable in trying to "debug" a program of the present complexity. The shifted and expanded body technique developed by Davis and Flügge-Lotz was used to compute the second-order effect of displacement thickness; however, this treatment is limited in applicability to the extreme forward portion of the body in question. Provisions were made in the program for considering both displacement speed and displacement pressure treatments (in the terminology of Van Dyke [15]), and Figs. II-1 and II-2 present results of these different treatments for vorticity and displacement effects on the paraboloid with respect to second-order wall shearing stress and heat transfer. It is seen that the displacement pressure treatment reduces the magnitude of the separate effects; this has been alluded to previously by various authors [8, 13, 14]. One fact is clear from study of these comparisons: second-order vorticity and displacement should properly be interpreted as a combined effect (vorticity-displacement interaction) and thereby remove the arbitrariness as to the treatment of the separate effects.

Shown in Fig. II-3 are the results obtained from a displacement speed and a displacement pressure treatment of second-order vorticity on the hyperboloid. Based on the results of a displacement speed treatment, Davis and Flügge-Lotz [8] conclude that the effects of vorticity on the second-order shear will continue to grow as s increases and eventually become a first-order effect. However, Fig. II-3 clearly shows that these conclusions are not justified when interpreted in a displacement pressure sense. This again points out that one should properly interpret vorticity and displacement in a combined sense as a vorticity-displacement interaction.

At this point one may well inquire as to which treatment (displacement speed or displacement pressure) is more appropriate for examination of the separate effects since, according to Van Dyke [15], one is free to choose either approach. As noted by Cheng [14] the displacement pressure treatment on a blunt body should yield results more in accord with the actual physical magnitude of the separate effects and hence is desirable from this standpoint. That such is true has been shown by Lewis [18] who presents a second-order displacement pressure treatment for vorticity on a sphere-cone as compared to a classical first-order boundary-layer analysis modified to include first-order vorticity effects. However, recent calculations have indicated that a

displacement pressure treatment for the separate effects of second-order vorticity and displacement yields nonunique solutions in that they are functions of the $\bar{N}$ value where the second-order matching conditions are applied. It is important to note that even though the separate effects have nonunique solutions, the sum of the separate effects, i.e., vorticity plus displacement, appears to yield a unique solution independent of the location of matching with the outer flow. Such is very interesting and has, to the best of the author's knowledge, not been previously recognized. Furthermore, the treatment of second-order vorticity and displacement in a combined sense (vorticity-displacement interaction) results in a unique solution independent of the value of $\bar{N}$. Hence, one is forced to conclude from these results that a displacement pressure treatment for the separate effects of second-order vorticity and displacement yields a nonunique solution, and thus these effects should properly be considered in a combined sense as a vorticity-displacement interaction.

That a displacement pressure treatment of the separate effects is inappropriate does not rule out the possibility of a displacement speed treatment. In fact, calculations have revealed that the separate second-order vorticity and displacement effects are indeed unique (independent of the $\bar{N}$ matching value) in a displacement speed approach. Hence, in view of the above results, it appears that the only correct way to consider the separate effects of second-order vorticity and displacement is in a displacement speed sense. Unfortunately, such a treatment results in unduly large values for each of the separate effects which are not representative of the actual physical magnitude and hence could lead to erroneous conclusions concerning the separate effects. This again points out that one should properly interpret second-order vorticity and displacement in a combined sense as a vorticity-displacement interaction.

For one to pursue the mathematical reason behind this interesting behavior, recourse should be taken to the governing second-order inner flow equations as given by Eqs. (2.48-2.49), Van Dyke [4]. In the limiting sense as $\bar{N} \to \infty$ the second-order matching conditions given by Eqs. (2.39-2.40), Van Dyke [4], should identically satisfy these governing equations; however, examination of these equations reveals that the only mathematically acceptable treatment for the separate effects of second-order vorticity and displacement is in a displacement speed sense. This is easily seen by considering the separate effect of second-order displacement. For this case the second-order matching conditions reduce to

$$\left.\begin{aligned}
&\bar{u}_1\,(\bar{s},\bar{N}) \sim \bar{U}_1\,(\bar{s},0)\\
&\bar{\rho}_1\,(\bar{s},\bar{N}) \sim \bar{R}_1\,(\bar{s},0)\\
&\bar{t}_1\,(\bar{s},\bar{N}) \sim \bar{T}_1\,(\bar{s},0)\\
&\bar{u}_2\,(\bar{s},\bar{N}) \sim \bar{U}_2\,(\bar{s},0)\\
&\bar{\rho}_2\,(\bar{s},\bar{N}) \sim \bar{R}_2\,(\bar{s},0)\\
&\bar{t}_2\,(\bar{s},\bar{N}) \sim \bar{T}_2\,(\bar{s},0)\\
&\partial\bar{u}_1\,(\bar{s},\bar{N})/\partial\bar{N} \sim 0\\
&\partial\bar{t}_1\,(\bar{s},\bar{N})/\partial\bar{N} \sim 0\\
&\partial\bar{u}_2\,(\bar{s},\bar{N})/\partial\bar{N} \sim 0\\
&\partial\bar{t}_2\,(\bar{s},\bar{N})/\partial\bar{N} \sim 0
\end{aligned}\right\}\quad \text{as } \bar{N} \to \infty \text{ considering second-order displacement only} \qquad \text{(II-1)}$$

so that the second-order inner flow momentum equation becomes, in the limit as $\bar{N} \to \infty$,

$$\left[\bar{R}_1\left(\bar{U}_1\frac{\partial\bar{U}_2}{\partial\bar{s}} + \bar{U}_2\frac{\partial\bar{U}_1}{\partial\bar{s}}\right) + \bar{R}_2\,\bar{U}_1\frac{\partial\bar{U}_1}{\partial\bar{s}}\right]_{\bar{n}=0} = -\,\bar{r}_w\,[\bar{R}_1{}^2\bar{T}_1\bar{S}_1'\bar{V}_2]_{\bar{n}=0}$$

$$+\left[\bar{R}_1\frac{\partial(\bar{U}_1\bar{U}_2)}{\partial\bar{s}} + \bar{R}_2\bar{U}_1\frac{\partial\bar{U}_1}{\partial\bar{s}}\right]_{\bar{n}=0} \qquad \text{(II-2)}$$

which is satisfied only if the term containing $\bar{S}_1'$ (the vorticity contribution) is not considered as a displacement effect. Such is precisely the condition for a displacement speed treatment. A similar argument holds with respect to the second-order inner flow energy equation with exactly the same conclusion regarding a displacement speed treatment. Hence one is forced by the mathematics of the theory to consider the separate second-order effects of vorticity and displacement in a displacement speed manner - a displacement pressure treatment is mathematically inconsistent with respect to the imposed second-order matching conditions. Such provides the answer to the nonuniqueness problem in the displacement pressure treatment discussed previously.

In summary, one must consider the separate effects of second-order vorticity and displacement in a displacement speed sense - a displacement pressure treatment results in a nonunique solution for each of the separate effects. However, a displacement speed treatment is unreasonable with respect to the magnitude of the separate effects and certainly not representative of the actual

physical effects. Hence, it appears that the proper interpretation of second-order vorticity and displacement is in a combined sense as a vorticity-displacement interaction and not as separate effects. Such an approach is adopted in the present paper.

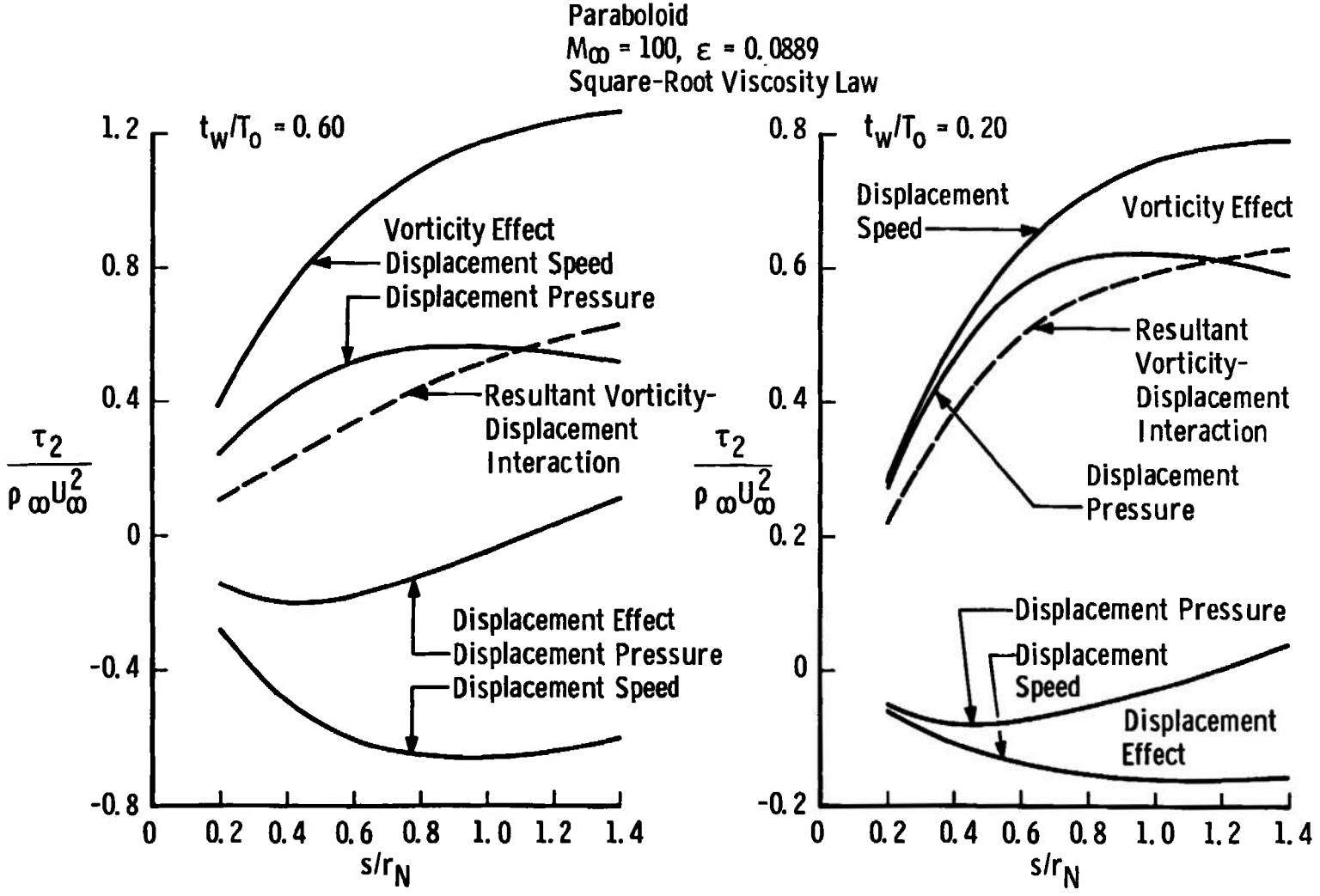

Fig. II-1 Effects of Vorticity and Displacement on Second-Order Wall Shearing Stress

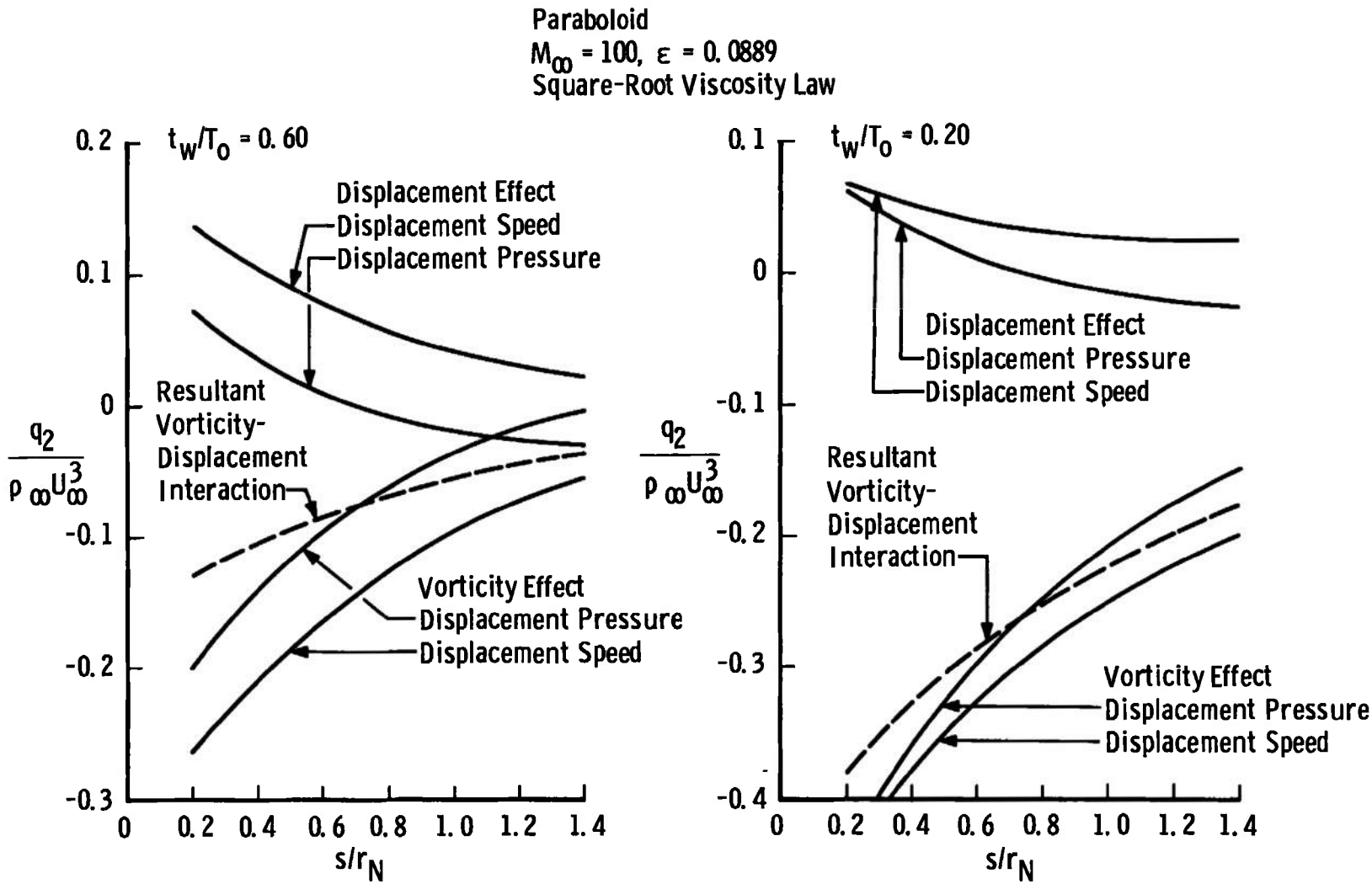

Fig. II-2 Effects of Vorticity and Displacement on Second-Order Wall Heat Flux

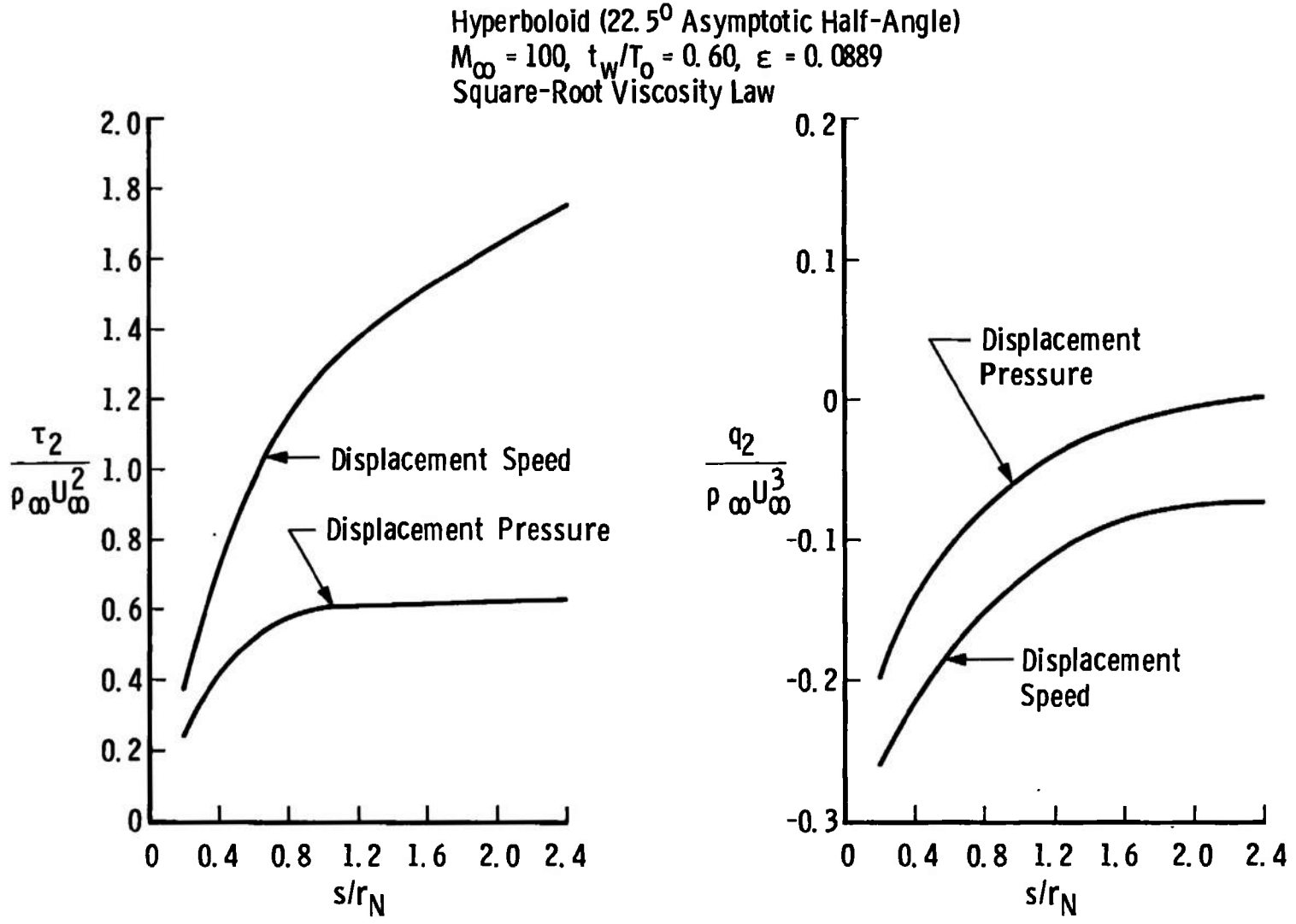

Fig. II-3 Second-Order Vorticity Treatment for Hyperboloid

APPENDIX III
DISPLACEMENT TREATMENT USING EFFECTIVE BODY TECHNIQUE

The shifted and expanded body technique developed by Davis and Flügge-Lotz [8] and used to obtain the results presented in Appendix I is extremely restrictive in that it is limited in use to the extreme forward portion of the body. Therefore, attention has been directed toward developing a more general method of treating the displacement effect which is valid over the entire body.*

Treatment of the second-order boundary-layer displacement effect requires the values of the second-order outer (inviscid) flow pressure, temperature, density, and tangential velocity at the surface of the physical body, i.e., $\bar{P}_2(\bar{s},0)$, $\bar{T}_2(\bar{s},0)$, $\bar{R}_2(\bar{s},0)$, and $\bar{U}_2(\bar{s},0)$. In order to obtain these quantities, one assumes that the basic outer (inviscid) flow has been calculated for both the original physical body and the effective body defined by the original body plus displacement thickness using, for example, numerical methods for solving the blunt body problem; the details of this calculation will be deferred until later in the discussion. Such an assumption provides the basic outer (inviscid) flow quantities on the surface of the physical body, e.g., $\bar{P}_1(\bar{s},0)$ $\bar{T}_1(\bar{s},0)$, etc., as well as on the surface of the effective body, e.g., $\bar{P}(\bar{s},\epsilon\bar{\delta}^*)$, $\bar{T}(\bar{s},\epsilon\bar{\delta}^*)$, etc. Following Davis and Flügge-Lotz [8], pp. 23-24, each quantity, say pressure $\bar{P}$ for example, is expanded in a Taylor series about the original physical body surface keeping terms through order ϵ to yield

$$\bar{P}(\bar{s},\epsilon\bar{\delta}^*) = \bar{P}_1(\bar{s},0) + \epsilon\bar{P}_2(\bar{s},0) + \ldots + \epsilon\bar{\delta}^* \frac{\partial\bar{P}_1(\bar{s},0)}{\partial\bar{n}} + \ldots \qquad \text{(III-1)}$$

so that, solving for the second-order term,

$$\bar{P}_2(\bar{s},0) = \frac{\bar{P}(\bar{s},\epsilon\bar{\delta}^*) - \bar{P}_1(\bar{s},0) - \epsilon\bar{\delta}^* \dfrac{\partial\bar{P}_1(\bar{s},0)}{\partial\bar{n}}}{\epsilon} \qquad \text{(III-2)}$$

where, from Eq. (2.20) of Van Dyke [4],

$$\frac{\partial\bar{P}_1(\bar{s},0)}{\partial\bar{n}} = -\bar{\kappa}\,\bar{R}_1(\bar{s},0)\,\bar{U}_1{}^2\,(\bar{s},0) \qquad \text{(III-3)}$$

---

*The present method was developed by Dr. R. T. Davis, currently at Virginia Polytechnic Institute, Blacksburg, Virginia, and follows the physical argument presented on pages 22-24 of the report by Davis and Flügge-Lotz [8].

Similar procedure is followed to obtain $\bar{T}_2(\bar{s},0)$, $\bar{R}_2(\bar{s},0)$, and $\bar{U}_2(\bar{s},0)$ where use of Eqs. (2.21) through (2.25), Van Dyke [4], is required to evaluate the normal derivative.

That the above technique is indeed compatible with the second-order theory of Van Dyke [4] may be shown by substituting the truncated (terms through order ϵ) series expressions into the first-order outer flow tangential momentum equation and treating the effective body surface as if it were a physical body, i.e.,

$$\frac{\partial \bar{P}(\bar{s}, \epsilon\bar{\delta}^*)}{\partial \bar{s}} + \bar{R}(\bar{s}, \epsilon\bar{\delta}^*)\ \bar{U}(\bar{s}, \epsilon\bar{\delta}^*)\ \frac{\partial \bar{U}(\bar{s}, \epsilon\bar{\delta}^*)}{\partial \bar{s}} = 0 \qquad \text{(III-4)}$$

which is just the conventional compressible Euler equation evaluated on the effective body surface. Equating terms of like power in ϵ and using consistency of first-order outer flow entropy and stagnation enthalpy along flow streamlines yields Eqs. (2.13b) and (2.18), Van Dyke [4], evaluated on the original body surface. Hence, this effective body treatment is compatible with the second-order theory of Van Dyke [4] and only limited by the capability of obtaining a valid first-order outer flow solution over the effective body. It should be noted, however, that the so-derived second-order quantities $\bar{P}_2(\bar{s},0)$, etc., are functions of ϵ and thus dependent on the numerical value of ϵ; this is in contrast to the shifted and expanded body treatment of Appendix II which is completely independent of ϵ. Hence, the results for second-order displacement cannot be scaled in terms of ϵ as can all the other second-order effects (which are independent of ϵ).

If one considers the practical details of this method, reference to the following sketch should prove helpful in defining various effective body parameters.

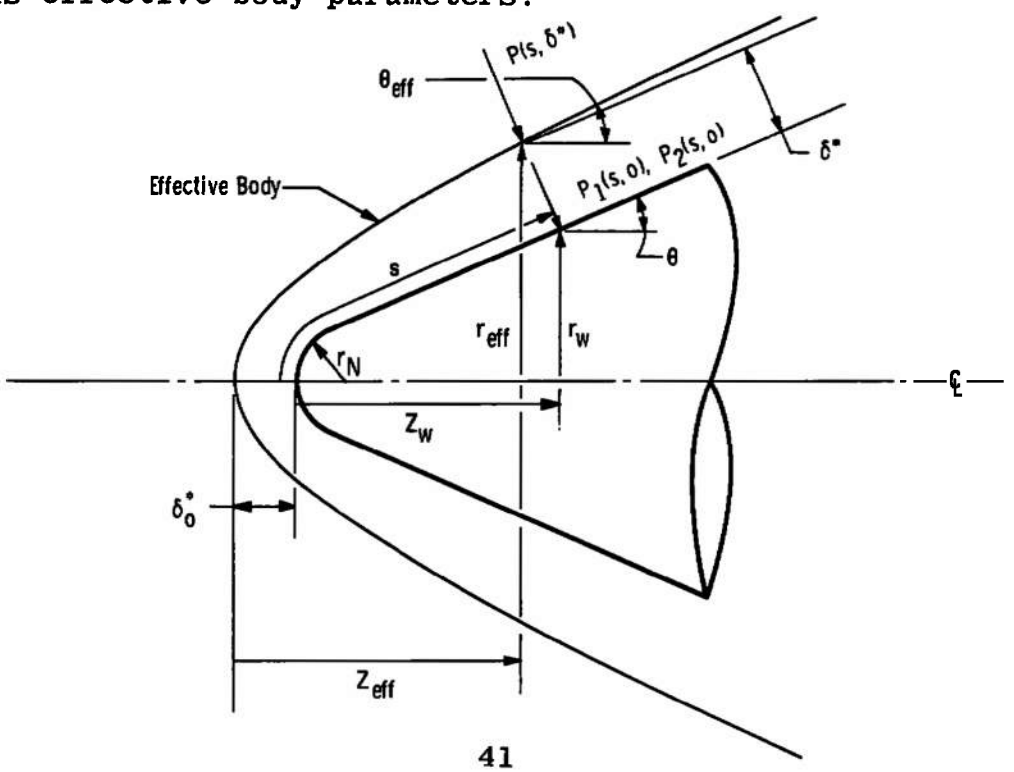

It is assumed that the displacement thickness distribution along the body is known from a first-order boundary-layer solution. Such an assumption enables the coordinates of the effective body to be defined by

$$\bar{r}_{eff} = \bar{r}_w + \epsilon\bar{\delta}^* \cos\theta \tag{III-5}$$

$$\bar{Z}_{eff} = \bar{Z}_w + \epsilon\bar{\delta}^*_o - \epsilon\bar{\delta}^* \sin\theta \tag{III-6}$$

which are in turn curve-fitted using a "walking" least-squares fit of the form

$$\bar{r}_{eff} = A\bar{Z}^B_{eff} \tag{III-7}$$

where A and B are determined in the least-squares sense. The fit is designed to be "walked" along the body in that, at any given body station, J stations in front of and behind the given station are used to obtain the A and B coefficients. For all calculations presented in this paper J = 3; experience has indicated that this value is sufficient since accurate fits through four significant figures to the right of the decimal have been obtained over the entire body.

Differentiating Eq. (III-7) yields

$$\tan\theta_{eff} = \frac{d\,\bar{r}_{eff}}{d\,\bar{Z}_{eff}} = AB\,\bar{Z}^{B-1}_{eff} \tag{III-8}$$

which determines the slope of the effective body geometry at a given location. Utilizing this information in conjunction with modified Newtonian theory yields the local pressure on the effective body surface according to the relation

$$\bar{P}(\bar{s}, \epsilon\bar{\delta}^*) = \frac{1}{\gamma M_\infty^2}\cos^2\theta_{eff} + \bar{P}'_o \sin^2\theta_{eff} \tag{III-9}$$

where an iteration procedure is used to locate the point of intersection of the normal from the physical body to the effective body at a given $\bar{s}$ location. In the above,

$$\bar{P}'_o = \frac{\left[\frac{(\gamma+1)M_\infty^2}{2}\right]^{\frac{\gamma}{\gamma-1}}\left[\frac{\gamma+1}{2\gamma M_\infty^2 - (\gamma-1)}\right]^{\frac{1}{\gamma-1}}}{\gamma M_\infty^2} \tag{III-10}$$

which is a modified form of the classical Rayleigh pitot formula.

Knowing the pressure from Eq.(III-9), one can determine the local tangential velocity and temperature on the effective body surface by

$$\bar{U}(\bar{s},\epsilon\bar{\delta}^*) = \left\{ 2\bar{T}_o \left[1 - \left(\frac{\bar{P}(\bar{s},\epsilon\bar{\delta}^*)}{\bar{P}'_o} \right) \right] \right\}^{1/2} \qquad \text{(III-11)}$$

$$\bar{T}(\bar{s},\epsilon\bar{\delta}^*) = \bar{T}_o - \frac{\bar{U}^2(\bar{s},\epsilon\bar{\delta}^*)}{2} \qquad \text{(III-12)}$$

under the restriction that the first-order outer flow be isentropic. Hence, all quantities needed in the effective body method discussed previously are now determined.

At this point a word of caution must be injected with respect to the above treatment. As is well-known, modified Newtonian theory is empirical in nature and not a mathematical solution to the governing first-order outer flow equations. Hence, the first-order outer flow equations used in the effective body method are not strictly applicable for use with modified Newtonian theory and cannot be justified in a rigorous sense for this application. To be strictly correct the first-order outer flow equations should be solved exactly using some numerical technique, say an inviscid blunt body and method of characteristics solution, over the effective body in question; such solutions have not been made in the present work. However, based on the agreement shown in Fig. 2, it is believed that modified Newtonian theory is an accurate approximation to the exact solution for the analytic bodies under consideration and hence acceptable for this application. Nevertheless, further work is needed to define the exact magnitude of this discrepancy.

APPENDIX IV

TABLE I

FREE-STREAM AND WALL CONDITIONS

M_∞	T_∞ [a]	γ	Pr	t_w/T_o [b]	Viscosity Law	Re_∞ [c]	ε [d]
10.0	100.0	1.40	0.70 or 1.00	0.20 or 0.60	Sutherland	400.00	0.1806
↓	↓	↓	↓	↓	Linear	1226.73	↓
↓	↓	↓	↓	↓	Square-Root	193.96	↓

a T_∞ has units of ^oK.

b Constant wall temperature

c $Re_\infty = (\rho_\infty U_\infty r_N)/\mu_\infty$

d ε is the perturbation parameter defined by Eq. (2.11), Van Dyke [4].

TABLE II

COMPARISON OF DRAG COEFFICIENTS ON PARABOLOID SHOWING EFFECTS OF VISCOSITY LAW, PRANDTL NUMBER, AND TYPE OF SOLUTION

Viscosity Law	Prandtl Number	Type of Solution	1st Order		1st and 2nd Order (All 2nd Order Effects Included)	
			C_{D_p}	C_{D_f}	C_{D_p}	C_{D_f}
Sutherland	0.70	Nonsimilar	0.1801	0.1045	0.2166	0.1798
Square-Root	0.70	Nonsimilar	0.1801	0.1108	0.2193	0.1962
Linear	0.70	Nonsimilar	0.1801	0.0725	0.2042	0.1070
Sutherland	1.00	Nonsimilar	0.1801	0.1057	0.2217	0.1819
Sutherland	0.70	Locally Similar	0.1801	0.1063		
Linear	1.00	Locally Similar	0.1801	0.0756		

Conditions: $M_\infty = 10.0$, $\varepsilon = 0.1806$, $\gamma = 1.40$, $t_w/T_0 = 0.20$

TABLE III

COMPARISON OF DRAG COEFFICIENTS INCLUDING SECOND-ORDER EFFECTS

Body	$\frac{t_w}{T_o}$	1st Order Solution		2nd Order Solution						Total	
		C_{D_p}	C_{D_f}	C_{D_p}	C_{D_f}					C_{D_p}	C_{D_f}
				DDS	VDI		TC	LC	STJ		
					VDS	DDS					
Paraboloid	0.20	0.1801	0.1045	0.0365	0.1403	-0.0759	0.0100	0.0017	-0.0008	0.2166	0.1798
					0.0644						
Paraboloid	0.60	0.1801	0.1127	0.0763	0.2744	-0.2070	0.0148	0.0042	-0.0050	0.2564	0.1941
					0.0674						
Hyperboloid (22.5° Asymptote)	0.20	0.3397	0.0708	0.0183	0.3122	-0.1557	0.0031	-0.0001	-0.0003	0.3580	0.2300
					0.1565						
Hyperboloid (22.5° Asymptote)	0.60	0.3397	0.0695	0.0395	0.5991	-0.4623	0.0045	0.0005	-0.0008	0.3792	0.2105
					0.1368						

Conditions: $M_\infty = 10.0$, $\varepsilon = 0.1806$, $\gamma = 1.40$, $Pr = 0.70$, Sutherland Viscosity Law

Legend: VDS External Vorticity, Displacement Speed Treatment
DDS Displacement, Displacement Speed Treatment
VDI Vorticity-Displacement Interaction
TC Transverse Curvature
LC Longitudinal Curvature
STJ Slip and Temperature Jump

Security Classification

DOCUMENT CONTROL DATA - R & D

(Security classification of title, body of abstract and indexing annotation must be entered when the overall report is classified)

1. ORIGINATING ACTIVITY (Corporate author)	2a. REPORT SECURITY CLASSIFICATION
Arnold Engineering Development Center ARO, Inc., Operating Contractor Arnold Air Force Station, Tennessee	UNCLASSIFIED
	2b. GROUP N/A

3 REPORT TITLE

HIGHER ORDER BOUNDARY-LAYER EFFECTS ON ANALYTIC BODIES OF REVOLUTION

4. DESCRIPTIVE NOTES (Type of report and inclusive dates)

September 1966 - September 1967 - Final Report

5. AUTHOR(S) (First name, middle initial, last name)

John C. Adams, Jr., ARO, Inc.

6. REPORT DATE	7a. TOTAL NO. OF PAGES	7b. NO. OF REFS
April 1968	55	18

8a. CONTRACT OR GRANT NO.	9a. ORIGINATOR'S REPORT NUMBER(S)
AF40(600)-1200 b. PROJECT NO. 8953 c. Program Element 6240533F d. 895303	AEDC-TR-68-57 9b. OTHER REPORT NO(S) (Any other numbers that may be assigned this report) N/A

10. DISTRIBUTION STATEMENT

This document has been approved for public release and sale; its distribution is unlimited.

11. SUPPLEMENTARY NOTES	12. SPONSORING MILITARY ACTIVITY
Available in DDC	Arnold Engineering Development Center, Air Force Systems Command, Arnold Air Force Station, Tennessee

13. ABSTRACT Results are presented from an investigation into second-order compressible boundary-layer theory applicable to blunt bodies formulated for numerical solution in the transformed plane using an implicit finite difference scheme. Various combinations of second-order effects (external vorticity, displacement, transverse curvature, longitudinal curvature, slip, and temperature jump) are considered for two different bodies: a paraboloid and a hyperboloid of 22.5-deg asymptotic half-angle, in a Mach 10 perfect gas flow under low Reynolds number conditions. It is shown that one should properly interpret second-order vorticity and displacement in a combined sense as a vorticity-displacement interaction; numerical results indicate that such interaction is the dominate second-order effect on the bodies under consideration, especially for the hyperboloid where it becomes a first-order effect. Caution is advised in the application of second-order theory to such bodies since the asymptotic matching conditions between inner and outer flow fields may not remain valid as the boundary layer grows while the external vortical (entropy) layer decreases in thickness.

DD FORM 1 NOV 65 1473

Security Classification

Security Classification

14. KEY WORDS	LINK A		LINK B		LINK C	
	ROLE	WT	ROLE	WT	ROLE	WT
2. boundary-layer theory						
blunt bodies						
second-order effects						
external voriticity						
displacement thickness						
transverse curvature						
longitudinal curvature						
slip						
temperature jump						
hypersonic flow						

1. Bodies of revolution - Boundary layer

1 - 2

Security Classification